Numerical Model of the Salt-Wedge Reach of the Duwamish River Estuary, King County, Washington

GEOLOGICAL SURVEY PROFESSIONAL PAPER 990

Prepared in cooperation with the Municipality of Metropolitan Seattle

Numerical Model of the Salt-Wedge Reach of the Duwamish River Estuary, King County, Washington

By Edmund A. Prych, W. L. Haushild, *and* J. D. Stoner

GEOLOGICAL SURVEY PROFESSIONAL PAPER 990

Prepared in cooperation with the Municipality of Metropolitan Seattle

UNITED STATES GOVERNMENT PRINTING OFFICE, WASHINGTON : 1976

UNITED STATES DEPARTMENT OF THE INTERIOR

THOMAS S. KLEPPE, *Secretary*

GEOLOGICAL SURVEY

V. E. McKelvey, *Director*

Library of Congress Cataloging in Publication Data

Prych, Edmund. A.
Numerical model of the salt-wedge reach of the Duwamish River Estuary, King County, Washington.

(Geological Survey Professional Paper 990)
Bibliography: p. 25-26.
Supt. of Docs. no.: I 19.16:990
1. Oceanography—Washington (State)—Duwamish River estuary—Mathematical models. 2. Estuarine pollution—Washington (State)—Duwamish River estuary—Mathematical models. 3. Phytoplankton—Washington (State)—Duwamish River estuary. I. Haushild, W. L., joint author. II. Stoner, J. D., joint author. III. Seattle. IV. Title. V. Series: United States Geological Survey Professional Paper 990.
GC856.P77 551.4'66'32 76-608136

For sale by the Superintendent of Documents, U.S. Government Printing Office
Washington, D.C. 20402

Stock Number 024-001-02886-7

CONTENTS

ILLUSTRATIONS

TABLES

DEFINITION OF SYMBOLS

A_i = average cross-sectional area of wedge element i, in square feet.

B_i = average width of interface between a wedge element i and the upper layer, in feet.

$BOD_{i,j}$ = 5-day biochemical oxygen demand of sublayer element i, j, in milligrams per litre.

$BOD'_{i,j}$ = 5-day biochemical oxygen demand of sublayer element i, j before a computation, in milligrams per litre.

BOD_f = 5-day biochemical oxygen demand of freshwater inflow to the estuary, in milligrams per litre.

BOD_M = miscellaneous 5-day biochemical oxygen demand added to the estuary downstream from First Avenue South Bridge, in pounds per day.

BOD_R = 5-day biochemical oxygen demand of Green River water at Tukwila gage, in milligrams per litre.

BOD_{RTP} = 5-day biochemical oxygen demand of Renton Treatment Plant effiuent, in milligrams per litre.

BOD_S = 5-day biochemical oxygen demand of seawater, in milligrams per litre.

BOD_T = miscellaneous 5-day biochemical oxygen demand added to the estuary upstream from First Avenue South Bridge, in pounds per day.

C = constituent concentration.

$C_{1/2}$ = constituent concentration when the Michaelis-Menton factor for that constituent equals 0.5.

C_i = constituent concentration in wedge element i.

C'_i = constituent concentration in wedge element i before computation.

$c_{i,j}$ = constituent concentration in sublayer element i, j.

$c'_{i,j}$ = constituent concentration in sublayer element i, j before a computation.

c_f = constituent concentration in freshwater inflow at wedge toe.

c_r = a coefficient used to compute incident long-wave radiation, dimensionless.

C_S = constituent concentration in seawater.

c_{t_j} = constituent concentration in water flowing into upstream end of sublayer j.

$CP_{i,j}$ = chlorophyll a concentration in sublayer element i, j, in micrograms per litre.

$CP'_{i,j}$ = chlorophyll a concentration in sublayer element i, j before a computation, in micrograms per litre.

CP_f = chlorophyll a concentration of freshwater inflow to the estuary, in micrograms per litre.

CP_S = chlorophyll a concentration of seawater, in micrograms per litre.

CP_{w_i} = chlorophyll a concentration in wedge element i, in micrograms per litre.

CP'_{w_i} = chlorophyll a concentration in wedge element i before a computation, in micrograms per litre.

D = upper layer thickness at the mouth of the estuary, in feet.

d_i = average thickness of a sublayer element in segment i, in feet.

DO_{BOD} = oxygen consumed per unit decay of biological oxygen demand, dimensionless.

DO_C = oxygen produced or consumed during a unit change in chlorophyll a concentration by growth or respiration, in milligrams oxygen per microgram chlorophyll a.

$DO_{i,j}$ = dissolved-oxygen concentration of sublayer element i, j, in milligrams per litre.

$DO'_{i,j}$ = dissolved-oxygen concentration of sublayer element i, j before a computation, in milligrams per litre.

$DO^s_{i,j}$ = dissolved-oxygen-saturation concentration of sublayer element i, j, in milligrams per litre.

DO_S = dissolved-oxygen concentration of seawater, in milligrams per litre.

DO_{w_i} = dissolved-oxygen concentration in wedge element i, in milligrams per litre.

DO'_{w_i} = dissolved-oxygen concentration in wedge element i before a computation, in milligrams per litre.

E = a constant of proportionality used in computing longitudinal mixing in wedge, dimensionless.

$E(T)$ = saturation vapor pressure in air at temperature T, in millibars.

E_a = vapor pressure in air, in millibars.

F_L = solar-radiation function in phytoplankton growth equation, dimensionless.

F_N = Michaelis-Menton factor for reducing the phytoplankton growth rate because of the deficiency of some constituent, dimensionless.

F_T = temperature function in phytoplankton growth equation, dimensionless.

G = growth rate of phytoplankton, in reciprocal hours.

G_o = maximum growth rate of phytoplankton, in reciprocal hours.

H = rate of heat transfer to water from atmosphere, in gram-calories per square centimetre per hour.

H_b = rate of heat transfer to water by evaporation, conduction, and outgoing long-wave radiation, when the water surface temperature is T_b, in gram-calories per square centimetre per hour.

H_L = rate of incoming long-wave radiation, in gram-calories per square centimetre per hour.

H_s = rate of solar energy penetrating water surface, in gram-calories per square centimetre per hour.

$H^*_{i,j}$ = solar energy passing through a unit area of the bottom of sublayer element i, j during a time step, in gram-calories per square centimetre.

i = a subscript denoting segment number.

i_{max} = number of segments in the estuary.

I_t = number of the time step.

j = a subscript denoting sublayer number.

K_{BOD} = decay rate for biochemical oxygen demand, in reciprocal days.

K^{20}_{BOD} = decay rate for biochemical oxygen demand at 20°C, in reciprocal days.

k = column subscript in volume transfer matrix.

k_C = change in solar-radiation attenuation coefficient per unit change in chlorophyll a concentration, in reciprocal feet per micrograms per litre.

$k_{i,j}$ = solar-radiation attenuation coefficient for sublayer element i, j, in reciprocal feet.

k^o_u = solar-radiation attenuation coefficient for upper layer in absence of phytoplankton, in reciprocal feet.

k^o_w = solar-radiation attenuation coefficient for wedge in absence of phytoplankton, in reciprocal feet.

k_{w_i} = solar-radiation attenuation coefficient for wedge element i, in reciprocal feet.

L = depth-averaged solar-radiation intensity in an element, in gram-calories per square centimetre per hour.

L_o = solar-radiation intensity for maximum phytoplankton growth, in gram-calories per square centimetre per hour.

N_t = number of time steps in a day.

P = atmospheric pressure, in millibars.

P_t = tidal-prism thickness, in feet.

$Q_{e_{i,j}}$ = upward flow through base of sublayer element i, j, in cubic feet per second.

Q_f = mean daily freshwater discharge into head of estuary, in cubic feet per second.

Q'_{fj} = fraction of Q_f that flows into sublayer j at toe of wedge, dimensionless.

$Q_{i,j}$ = flow rate into the upstream face of sublayer element i, j, in cubic feet per second.

Q_R = mean daily discharge of Green River at Tukwilla gage, in cubic feet per second.

Q_{RTP} = mean daily discharge of effluent from Renton Treatment Plant, in cubic feet per second.

Q_s = rate at which saltwater leaves the wedge and is transported upstream from the toe, in cubic feet per second.

Q'_{sj} = fraction of Q_s that returns to sublayer j at the toe of the wedge, dimensionless.

R = phytoplankton respiration rate, in reciprocal hours.

R_{20} = phytoplankton respiration rate at 20°C, in reciprocal hours.

R_a = the mean daily relative humidity, in percent.

R_{v_i} = the lesser of the volume ratio V_{i+1}/V_i and unity, dimensionless.

R'_{v_i} = the lesser of the volume ratio V_i/V_{i+1} and unity, dimensionless.

r = atmospheric-reaeration coefficient, in reciprocal days.

$S_{i,j}$ = salinity of sublayer element i, j, in parts per thousand.

S_o = slope of the interface between wedge and upper layer in feet per foot.

S_R = total daily incident solar radiation. in gram-calories per square centimetre.

S'_R = fractional amount of total solar radiation penetrating water surface, dimensionless.

T_a = mean daily air temperature, in degrees Celsius.

T_b = a reference temperature, in degrees Celsius.

$T_{i,j}$ = temperature of sublayer element i, j, in degrees Celsius.

$T'_{i,j}$ = temperature of sublayer element i, j before a computation, in degrees Celsius.

T_s = water-surface temperature, in degrees Celsius.

T_{w_i} = temperature of wedge element i, in degrees Celsius.

T'_{w_i} = temperature of wedge element i before a computation, in degrees Celsius.

U = volume-transfer matrix for a sublayer, in cubic feet.

$U_{i,k}$ = term in matrix U which equals volume in sublayer element i, j at the end of a time step that was in element $(i-10+k), j$ at beginning of the time step, in cubic feet.

U_e = entrainment volocity across the interface between wedge and upper layer, in feet per second.

U'_{ej} = vertical velocity at base of sublayer j divided by entrainment velocity, U_e, dimensionless.

V_i = volume of a wedge element, in cubic feet.

V'_i = volume of a wedge element for a preceding time step, in cubic feet.

V_{s_i} = volume of a sublayer element, in cubic feet.

V'_{s_i} = volume of a sublayer element in preceding time step, in cubic feet.
v_i = velocity of water in top sublayer relative to water in wedge, in feet per second.
W_a = mean daily wind speed, in feet per second.
w = settling velocity of phytoplankton, in feet per second.
x = longitudinal coordinate measured upstream from estuary mouth, in feet.
x_a = longitudinal coordinate of a cross section bounding a volume that shall move into a sublayer element (see fig. 5), in feet.
x_b = longitudinal coordinate of a cross section bounding a volume that shall move into a sublayer element (see fig. 5), in feet.
x_{m_i} = longitudinal coordinate of center of wedge element i, in feet.
x_t = longitudinal coordinate of wedge toe, in feet.
x_{u_i} = longitudinal coordinate of downstream face of wedge element i, in feet.
x'_{u_i} = longitudinal coordinate of the downstream face of wedge element i, for preceding time step, in feet.
α = latent heat of vaporization at 0°C, in gram-calories per gram.
β = change in latent heat of vaporization per unit change in temperature in gram-calories per gram per degree Celsius.
γ = constant in the Bowen ratio relating heat transfer by conduction to that by evaporation, dimensionless.
$\Delta BOD_{i,j}$ = change in biochemical oxygen demand of sublayer element i, j due to decay during a time step, in milligrams per litre.
ΔC_i^{i+1} = change during a time step in concentration of a constituent in wedge element i due to mixing with water from element $i+1$.
$\Delta CP_{i,j}$ = change in chlorophyll a concentration in sublayer element i, j due to growth and respiration during a time step, in micrograms per litre.
ΔCP_{w_i} = change in chlorophyll a concentration in wedge element i due to growth and respiration during a time step, in micrograms per litre.
ΔDO_w = oxygen-consumption rate in wedge, in milligrams per litre per hour.
Δx_i = length of a wedge element i, in feet.
Δt = length of time step in finite difference model, in seconds.
δ = difference between kelvin and Celsius temperature scales, in degrees.
ϵ = emissivity of water, dimensionless.
ϵ_y = vertical turbulent diffusion coefficient between sublayers, in square feet per second.
ζ = constant in equation for saturation vapor pressure, dimensionless.
η = constant in equation for saturation vapor pressure, in degrees kelvin.
θ = time angle, in radians.
λ = mass transfer coefficient for evaporation in grams per square centimetre per hour per millibar per foot per second.
ξ = constant in equation for saturation vapor pressure, in millibars.
σ = Stefan-Boltsman constant, in gram-calories per square centimetre per hour per degree kelvin.

ENGLISH-METRIC EQUIVALENTS

Multiply	*By*	*To obtain*
feet (ft)	0.3048	metres (m)
square feet (ft^2)	.0929	square metres (m^2)
cubic feet (ft^3)	.02832	cubic metres (m^3)
feet per second (ft/s)	.3048	metres per second (m/s)
square feet per second (ft^2/s)	.0929	square metres per second (m^2/s)
cubic feet per second (ft^3/s)	.02832	cubic metres per second (m^3/s)
miles (mi)	1.609	kilometres (km)
pounds per day (lb/day)	.4536	kilograms per day (kg/day)

NUMERICAL MODEL OF THE SALT-WEDGE REACH OF THE DUWAMISH RIVER ESTUARY, KING COUNTY, WASHINGTON

By EDMUND A. PRYCH, W. L. HAUSHILD, and J. D. STONER

ABSTRACT

A numerical model of a salt-wedge estuary developed by Fischer (1974) has been expanded and used to calculate the distributions of salinity, temperature, chlorophyll *a* concentration, biochemical oxygen demand, and dissolved-oxygen concentration in the Duwamish River estuary, King County, Wash. With this model, which was calibrated and verified with observed data, computed temperatures usually agreed within 2° Celsius of observed temperatures. During a phytoplankton bloom in the summer of 1968, the computed chlorophyll *a* concentrations increased and decreased with the observed concentrations; however, during two blooms in 1967 the computed high concentrations persisted farther downstream and lasted a few days longer than the observed concentrations. The computed and observed dissolved-oxygen concentrations usually agreed within 2 milligrams per litre, except during phytoplankton blooms. During the blooms, the differences were often larger, especially when the computed chlorophyll *a* concentrations were larger than the observed concentrations.

The model was used to predict the dissolved-oxygen concentrations in the Duwamish River estuary when the Renton Treatment Plant sewage-effluent discharge is increased to its proposed maximum of 223 cubic feet per second (6.31 cubic metres per second). The computed monthly average dissolved-oxygen concentrations in the estuary decreased by a maximum of 2 milligrams per litre when compared with computations for the summer of 1971, when the effluent discharge averaged 37 cubic feet per second (1.05 cubic metres per second). The increase in effluent discharge is not expected to cause large changes in phytoplankton concentrations in the estuary.

INTRODUCTION

This report describes a numerical model designed for predicting concentrations of DO (dissolved oxygen) and other constituents in the Duwamish River estuary, a salt-wedge estuary (fig. 1). Modeling the upper layer (the layer overlying the salt wedge) is emphasized, but because concentrations of constituents in the wedge affect those in the upper layer, modeling of the salt wedge also is described.

Earlier, Fischer (1974) presented a generalized numerical model for predicting constituent concentrations in salt-wedge estuaries. Stoner, Haushild, and McConnell (1974) then used Fischer's model to predict DO concentrations in the salt wedge of the Duwamish River estuary. They verified the model with observed DO concentrations in the wedge and with observed salinity distributions in the upper layer. In the present study, the model for the Duwamish River estuary was extended to predict DO concentrations in the upper layer of the Duwamish River estuary. To accomplish this goal, it is necessary for the model to also predict the temperature, the 5-day BOD (biochemical oxygen demand), and the phytoplankton concentrations in the estuary.

This report is one of several resulting from a study of the effects on estuary water quality of changes in the treatment and the quantity of sewage discharged to the Duwamish River estuary. The effects of effluent from RTP (Renton Treatment Plant), which provides secondary treatment, are of particular interest. The study is being conducted by the U.S. Geological Survey in cooperation with Metro (Municipality of Metropolitan Seattle). As part of its general plan for the treatment and disposal of sewage from the Metropolitan Seattle area, Metro operates the RTP and relies on the Duwamish River estuary to transport an increasing quantity of RTP effluent to Elliott Bay and Puget Sound. If the RTP effluent is detrimental to the estuary water quality—especially for its use by anadromous fish—regulatory Federal and State agencies may prohibit or limit the discharge of the effluent and (or) require additional treatment of the sewage at the plant. A primary reason for developing the mathematical model of this report was to predict the effects of proposed changes in the quantity and quality of the RTP effluent on the estuary water quality.

The estuary reach included in the model study extends from the estuary mouth to the wedge toe. The wedge toe is defined as the upstream limit of a specified salinity. The location of the toe depends on tide stage and river discharge; therefore, the location of the model's upstream boundary is a function of time. During the summer low-flow periods, the toe ranges from a little downstream of 16th Avenue South Bridge to a little downstream of East Marginal Way Bridge. (See fig. 1.) The distance from the mouth to the wedge toe during the low-flow periods averages about 5 mi (8 km). All flows are computed by using equations for the conservation of fluid volume and empirical formulas

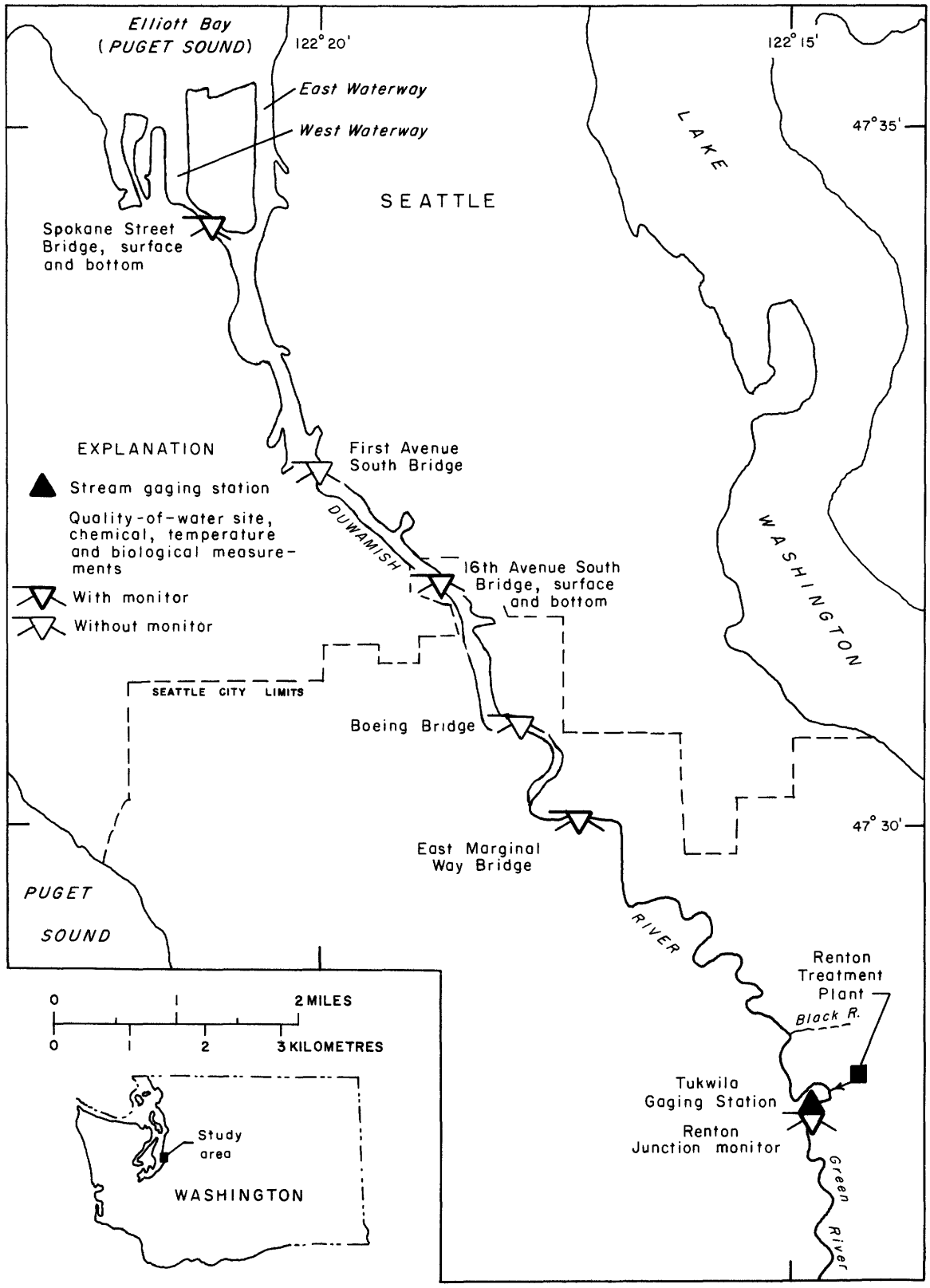

FIGURE 1.—Green-Duwamish River study area.

developed from data for the Duwamish River estuary; the dynamic equations of motion are not used. The wedge is assumed to be vertically and laterally homogeneous. The upper layer is divided into three sublayers that are also assumed to be vertically and laterally homogeneous. Resolution of constituent concentrations in the longitudinal direction is limited by the length of the segments into which the estuary is divided; segment lengths average about 600 ft (200 m).

The model of the Duwamish River estuary was verified by data from the June-September periods of 1967–69 and 1971. The summer months are periods of low river discharges when the probability of low DO concentrations are highest. Finally, the model was used to predict constituent concentrations in the estuary in the future when the discharge from RTP is expected to be much larger than at present.

Information on river discharges, salinities, and other constituent concentrations, and physical characteristics of the Duwamish River estuary are given in several previous reports, including Dawson and Tilley (1972), Santos and Stoner (1972), Stoner (1972), Stoner, Haushild, and McConnell (1974), and Welch (1969). The interested reader is referred to these reports for background information and data other than that included in this report.

ACKNOWLEDGMENTS

The authors express their appreceiation to Glen D. Farris, superintendent, Water Quality and Industrial Waste Division, Municipality of Metropolitan Seattle, and his staff for contributing information and many data needed for the model study and for their continuing support and encouragement in the study of the estuary's water quality. The authors acknowledge the contribution made by Hugo B. Fischer, Professor of Civil Engineering, University of California at Berkeley and part-time employee of the U.S. Geological Survey, in conceiving and developing the salt-wedge estuary model subsequently useful in modeling the Duwamish River estuary and for advice in development of the present model. An interim version of a computer program for constituent transport in the upper layer of the Duwamish River estuary, by Richard H. French, graduate student at the University of California at Berkeley, expedited the development of the present Duwamish River estuary model. The authors depended considerably on K. V. Slack of the U.S. Geological Survey for guidance and advice in modeling the phytoplankton and their effects on dissolved oxygen, for suggestions about presenting the results of the study of phytoplankton and herbivores, and for furnishing literature pertinent to the biological modeling. The authors also thank H. E. Jobson, and M. J. Sebetich of the Geological Survey for reviewing this manuscript and for their constructive criticisms.

FLOW MODEL

GENERAL DESCRIPTION

Fischer (1974) developed the general salt-wedge estuary model which was used in the present study. The typical salt-wedge estuary is characterized by a lower layer, or wedge, of nearly undiluted seawater of uniform salinity. For the Duwamish River estuary, the term "sea" is interpreted as Elliott Bay (fig. 1), the body of water outside the mouth of the estuary.

Figure 2 shows observed salinity, temperature, and DO-concentration distributions in the Duwamish River estuary. The wedge in the Duwamish River estuary is defined as that volume of water with a salinity greater than 25 ppt (parts per thousand). By comparison, the salinity of the water flowing into the estuary from Elliott Bay is about 28 ppt. The 25 ppt salinity was chosen because the locus of points with this salinity was fairly easy to define and is a good approximation of the interface between the nearly homogeneous wedge and the stratified upper layer. The interface is

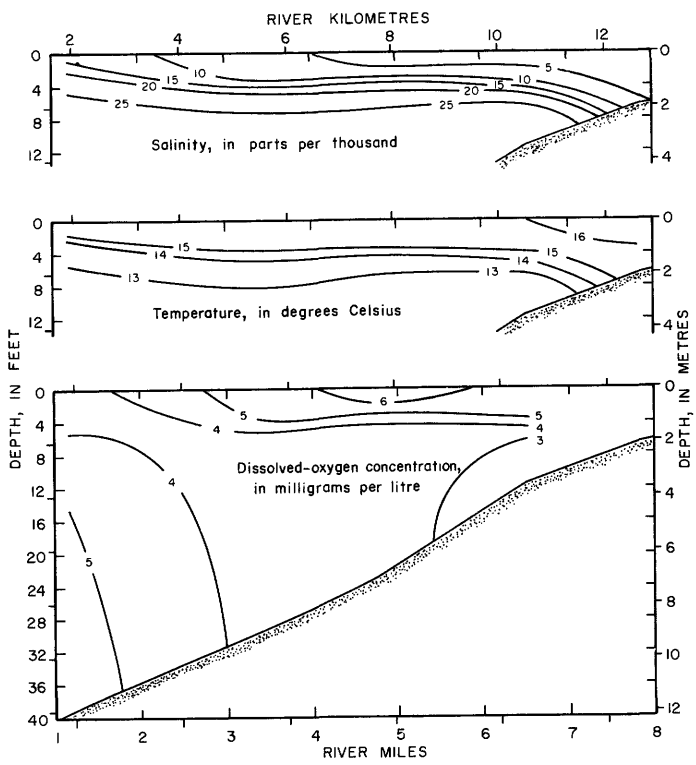

FIGURE 2.—Observed longitudinal profiles of salinity, temperature, and dissolved-oxygen concentration in Duwamish River estuary during the low high tide of September 13, 1968.

relatively stable except near the toe. The location of the toe, defined as the upstream extent of the 25 ppt salinity, was fairly easy to define; however, the upstream extent of salinities slightly less than 25 ppt moved erratically, suggesting more intense mixing upstream from the toe.

Stoner (1972) found that during a tidal cycle, saltwater in the wedge near the toe flows upstream at a net rate of about 200 ft^3/s (5.7 m^3/s). This saltwater is transported upstream from the wedge toe, is mixed vertically, and is returned through the upper layer to the sea. The increase in salinity of the upper layer toward the sea (fig. 2) suggests entrainment from the wedge to the upper layer over the entire interface. A nearly uniform salinity in the wedge, approximately equal to that in Elliott Bay, indicates that freshwater is not transferred into the wedge from the upper layer. The net circulation pattern in the estuary is probably as shown in figure 3.

The waters in both the upper layer and the wedge oscillate upstream and downstream in the estuary during a rising and falling tide. In addition, water in the upper layer has a net downstream motion because the upper layer carries to the sea both the water discharged to the estuary by the river and the water entrained from the wedge. Water in the wedge has a net upstream motion because the wedge loses water to the upper layer by entrainment. Thus, water entering the upper layer is transported to the sea, and on its way it is mixed with water entrained from the wedge. Water entering the wedge on a rising tide either returns to the sea on a falling tide or remains in the wedge and moves upstream until it is entrained into the upper layer, where it then is returned to the sea. In addition to these advective transport processes there also are dispersive transport processes in the estuary; they are discussed in the section "Transport model."

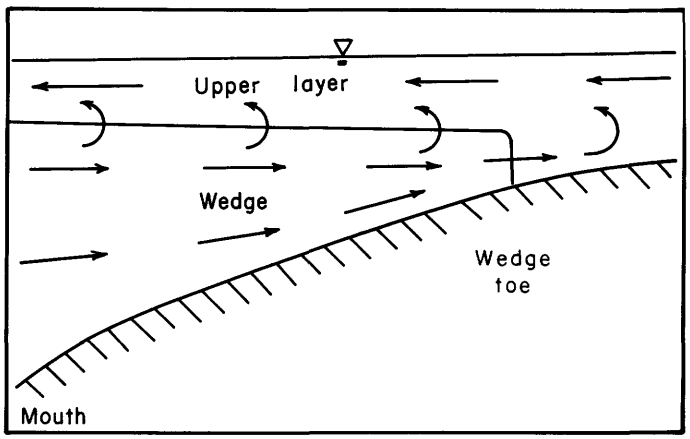

FIGURE 3.—Probable circulation pattern in Duwamish River estuary. Arrows indicate direction of mean flow.

For purposes of computation, the estuary is divided into control volumes called elements (fig. 4). The elements are constructed by first dividing the estuary vertically into the wedge and the upper layer, and the upper layer is in turn divided into three equal-depth sublayers. Next, the estuary is divided longitudinally by vertical planes that are perpendicular to the longitudinal axis of the estuary. Each volume between adjacent vertical planes is called a segment and contains one wedge element and three sublayer elements. Typically, there are about 35 segments in the estuary. The segments are numbered longitudinally from the toe to the mouth ($i=1$ to i_{max}), and the sublayers are numbered vertically from bottom to top ($j=1,2,3$).

All segments move with the velocity of the wedge water so that there is no net flow between wedge elements. However, because of the relative motion between the water in the wedge and the water in the sublayers, there is a net flow across the vertical boundaries between elements in the sublayers.

All horizontal flows are computed from conservation of volume equations for the water. Input information required for computing water flow in the model includes the geometry of the estuary, location of the wedge toe, flow rates across the vertical boundary at the wedge toe, vertical entrainment velocities, elevation of the water surface, thickness of the upper layer at the estuary mouth, and the slope of the interface.

In this, as in most numerical models, computations are made for finite steps in time, Δt. This model uses time steps of 15 minutes. The model computes average flow, mixing and other process rates, and the resulting changes in constituent concentrations during each time step.

FLOW IN THE WEDGE

In the model, the water surface is assumed to remain

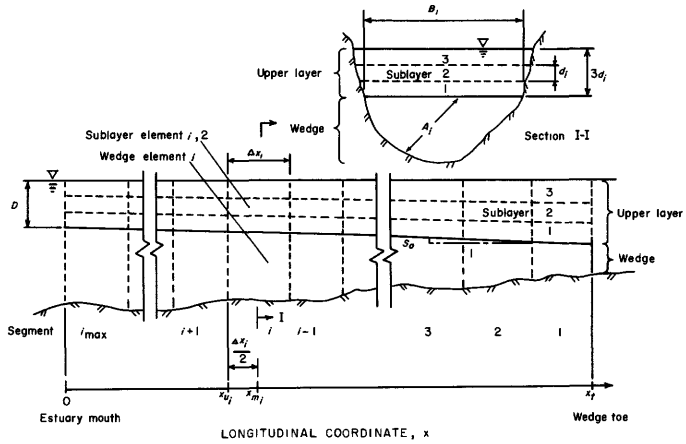

FIGURE 4.—Schematic diagram defining elements in Duwamish River estuary model. See text for definition of symbols.

horizontal and the interface is assumed to have a constant slope, S_o, at all times. During a given day, the upper-layer thickness at the mouth, D, is assumed to be constant even though the wedge becomes deeper and shallower with a rising and falling tide. The wedge toe moves upstream and downstream with the tide. Data from the estuary show that these are reasonable assumptions for the periods modeled in this study.

At the start of computations for a time step, the new space occupied by the wedge is filled with the wedge elements from the end of the preceding time step. These elements, or water volumes, are deformed to fit the wedge geometry for the time step. Starting with segment number one at the toe, the model calculates for each wedge element a new length Δx_i, new longitudinal coordinates of the center x_{mi}, and downstream face x_{u_i}, a new average cross-sectional area A_i, and a new average interface width B_i. The model computes the widths, areas, and other geometrical properties by interpolation between data at reference cross sections where the channel geometry is defined by input data. If the total volume of all the previously designated wedge elements is insufficient to fill the wedge, a new element of seawater is added at the estuary mouth. On the other hand, if the wedge is filled before all the designated elements are used, the fluid in the extra elements is assumed to have flowed into the sea, and the model deletes these downstream elements from the computations.

Whenever the number of wedge elements exceeds 50, or whenever the shortest wedge element is less than 200 ft (60 m) long, the number of wedge elements is decreased by combining the shortest element with its shortest neighbor. Also, the element adjacent to the wedge toe is combined with its neighbor whenever its volume is less than the volume that would flow out of it during the time step. The corresponding sublayer elements of two segments are combined at the same time the wedge elements are combined.

Near the end of all computations associated with a time step, the volume of each wedge element is decreased to account for entrainment. The model makes the calculation,

$$V_i = V'_i - U_e B_i \Delta x_i \Delta t, \tag{1}$$

where V'_i and V_i are the wedge-element volumes before and after this subtraction is made, and U_e is the entrainment velocity across the interface. In addition, the volume of the wedge element adjacent to the toe is decreased by the amount $Q_s \Delta t$, where Q_s is the net upstream flow rate of saltwater in the wedge in the vicinity of the toe.

Because the elements in the wedge move with the water, there is no net flow across the boundaries between wedge elements. However, longitudinal constituent transport between wedge elements may occur by longitudinal dispersion; the modeling of this process is discussed in the section "Transport in the Wedge."

FLOW IN THE UPPER LAYER

The location and length of the elements in the sublayers are determined by the geometry of the elements in the wedge. The thickness, d_i, of each sublayer element in a segment is the same:

$$d_i = (D + S_o x_{m\,i})/3. \tag{2}$$

For simplicity, the widths of all sublayer elements in a segment are assumed to equal the interface width B_i. The volume, $V_{s\,i}$, of a sublayer element is therefore given as

$$V_{s\,i} = \Delta x_i B_i d_i. \tag{3}$$

Because of the relative motion between the water in the wedge and the water in the upper layer, there is usually a net flow between adjacent elements in a sublayer. An expression for the flow between elements in a sublayer is obtained by writing an equation for the conservation of water volume for a sublayer element. The resulting expression is

$$Q_{i+1,j} = Q_{i,j} + (Q_{e_{i,j}} - Q_{e_{i,j+1}}) + \frac{(V'_{s\,i} - V_{s\,i})}{\Delta t}, \tag{4}$$

where $Q_{i,j}$ is the flow rate into the upstream face of sublayer element i, j; $Q_{e,j}$ is the upward flow through the base of element i, j; and $V'_{s\,i}$ and $V_{s\,i}$ are the volumes of the sublayer element for the preceding and present times steps, respectively. The upward flows $Q_{e\,i,j}$ are computed with the relation

$$Q_{e\,i,j} = U'_{e\,j} U_e \Delta x_i B_i, \tag{5}$$

where $U'_{e\,j}$ is the vertical velocity at the base of sublayer j divided by the entrainment velocity across the interface U_e. Vertical flow through the water surface is prevented by defining $U'_{e\,4} = 0$.

The use of equation 4 requires inflow to each sublayer at the wedge toe $Q_{1,j}$. The model uses

$$Q_{1,j} = Q'_{f\,j} Q_f + Q_{s\,j} Q_s, \tag{6}$$

where Q_f is the mean daily discharge of freshwater into the head of the estuary, and $Q'_{f\,j}$ and $Q'_{s\,j}$ are the fractions of Q_f and Q_s that flow into sublayer j.

The parameters U_e, $U'_{e\,j}$, $Q'_{f\,j}$, and $Q'_{s\,j}$ are input information to the model. The selection of numerical values for these and other parameters for the Duwamish River estuary is discussed in the section "Input Data."

TRANSPORT MODEL

GENERAL DESCRIPTION

This section describes the procedures used in the model to calculate changes in constituent concentrations due to advection and diffusion. The effects of other processes on constituent concentrations, such as the effects of photosynthesis on DO concentration and of solar radiation on temperature, are discussed in the section "Constituent Models."

The water-transport processes modeled are longitudinal advection and dispersion in the wedge, entrainment from the wedge to the upper layer and from each sublayer to the sublayer above (vertical advection), vertical turbulent diffusion in the upper layer and longitudinal advection in the upper layer. The assumption of lateral and vertical homogeneity in the wedge prohibits modeling vertical or lateral transport processes within the wedge, and the assumption of lateral homogeneity in the upper layer prohibits modeling lateral transport processes there.

That part of the longitudinal dispersion in the upper layer that is caused by the combined action of vertical differences in velocity and vertical mixing is represented in the model because both these phenomena are modeled; whereas, that part of the longitudinal dispersion that is caused by the action of lateral differences in velocity and lateral mixing is not modeled explicitly. However, the finite-difference representations of the advective processes in the model introduce additional longitudinal dispersion in the upper layer; this additional dispersion is often called "numerical dispersion." (For example, see Bella and Grenney, 1970.)

During each time step the model computes the changes in concentrations due to transport and other processes one at a time. The calculations are performed in the following order:

1. Position elements in the wedge.
2. Change concentrations in the wedge to account for longitudinal dispersion in the wedge.
3. Change concentrations in the upper layer to account for entrainment from the wedge and advection in the upper layer.
4. Change concentrations in the upper layer to account for vertical diffusion.
5. Change concentrations in the wedge and the upper layer to account for processes other than water transport.

TRANSPORT IN THE WEDGE

After the positions of the elements in the wedge are determined by the method described previously in the section "Flow in the Wedge," the model need only calculate changes in constituent concentrations due to longitudinal dispersion. No advection calculations are required for the wedge because there is no net flow between wedge elements.

The model computes the changes due to dispersion with a procedure developed by Fischer (1972, 1974). The change in concentration caused by the mixing between adjacent wedge elements during a time step is assumed proportional to the width of the elements and to the distance traveled by the elements during the time step and inversely proportional to the square of the element lengths. The change in constituent concentration, ΔC_i^{i+1}, of wedge element i due to mixing with water from element $i+1$ is calculated as

$$\Delta C_i^{i+1} = R_{V_i} (C'_{i+1} - C'_i) \left[2E(B_i + B_{i+1}) \left| x_{u_i} - x'_{u_i} \right| / (\Delta x_i + \Delta x_{i+1})^2\right], \quad (7)$$

where E is a dimensionless constant of proportionality with a value of about 0.2; x_{u_i} and x'_{u_i} are longitudingal coordinates of the boundary between wedge elements i and $i+1$ for the present and previous time steps, respectively; C'_i is the constituent concentration in wedge element i before the dispersion computation; and R_{V_i} is the lesser of V_{i+1}/V_i and unity. To avoid occasional instabilities in the computations, an upper limit of 0.5 is imposed on the term in square brackets in equation 7. The corresponding change in concentration of a constituent in wedge element $i+1$ due to mixing with water from wedge element i is

$$\Delta C_{i+1}^{i} = -\Delta C_i^{i+1} R'_{V_i} / R_{V_i}, \quad (8)$$

where R'_{V_i} equals the lesser of the values V_i/V_{i+1} and unity.

After calculating the quantities ΔC_i^{i+1} and ΔC_i^{i+1} for all i, the model computes a new constituent concentration, C_i, for each wedge element, using the expression

$$C_i = C'_1 + \Delta C_i^{i+1} + \Delta C_i^{i'-1}, \quad (9)$$

where C'_i and C_i are constituent concentrations before and after this computation.

TRANSPORT IN THE UPPER LAYER

ADVECTION

The present model treats longitudinal advection a little differently than does the original model of Fischer (1974). The present model uses an extension of the upstream difference scheme or the method of characteristics that is computationally stable when a water particle moves more than one element length during a time step.

The model computes a volume transfer matrix, U, of

dimension i_{max} by 21, for each sublayer. Each term $U_{i,k}$ in the matrix equals the volume in element i,j at the end of a time step that was advected horizontally from element $(i-10+k)$, j during the time step (fig. 5). Presently, the movement of water is limited to nine elements in the downstream (k=1–9) or upstream (k=11–19) directions. The term with the subscript k=10 is the volume that remains in element i during the time step. Terms with k=20 and 21 represent volumes that originate seaward of the estuary mouth and upstream of the wedge toe, respectively.

The model evaluates terms in a row of the matrix U as follows. If the flow is into the upstream face of sublayer element i,j ($Q_{i,j}>0$), one sums the sublayer volumes from the preceding time step, V'_s, either wholly or in parts, upstream from the element until the accumulated volume equals the inflow volume $Q_{i,j}\Delta t$. If the upstream boundary of the model is reached before the desired volume is obtained, a temporary element with sufficient volume to make up the deficit is attached to the upstream end of the sublayer. Starting at x_a—the location of the cross section at the end of the accumulated volume in figure 5—the volumes V'_s are summed again, this time proceeding in the downstream direction until the accumulated sum equals $V_{s\,i}-(Q_{e\,i,j}-Q_{e\,i,j+1})\Delta t$, or until the upstream face of element i is reached. The location of the cross section at the end of this summation is designated as x_b. The parts of the volumes V'_s contained in the interval x_b to x_a are assigned to the appropriate terms in $U_{i,k}$. If flow is into the downstream face of element i,j ($Q_{i+1,j}<0$), similar computations are performed on the elements downstream from element i,j.

The volume remaining in an element during a time step, $U_{i,10}$, is computed by subtracting the outflow volumes from the element volume and assuring that the difference is not negative:

$$U_{i,10} = V'_s - 0.5\,(Q_{i+1,j} + |Q_{i+1,j}| - Q_{i,j} + |Q_{i,j}|)\Delta t \qquad (10a)$$

or

$$U_{i,10} = 0 \text{ if the above is negative} \qquad (10b)$$

With the above information the constituent concentrations can be changed to account for advection during a time step. The program uses the equation,

$$c_{i,j} = (Q_{e_{i,j}}\Delta t\ c'_{i,j-1} - Q_{e\,i,j+1}\ \Delta t\ c'_{i,j} + U_{i,20}\ C_S + U_{i,21}\ c_{t_j} + \sum_{k=1}^{19} U_{i,k}\ c'_{i-10+k,j})\,/V_{s_i}, \qquad (11)$$

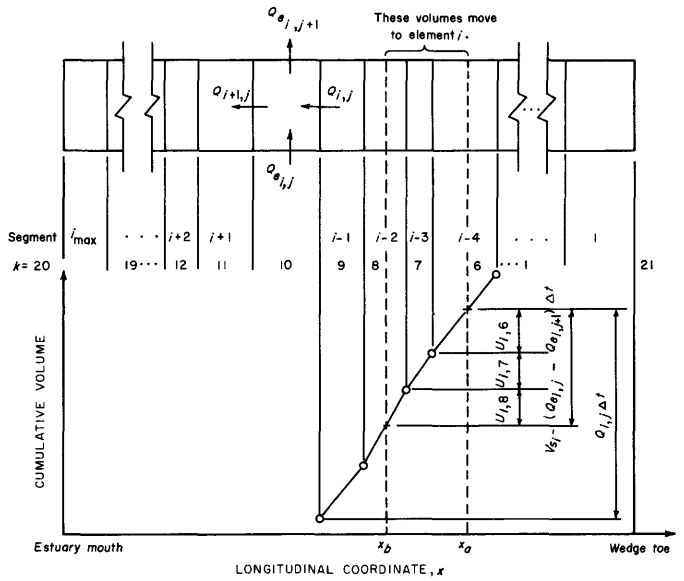

FIGURE 5.—Elements in the volume-transfer matrix, U. See text for definition of symbols.

where $c'_{i,j}$ and $c_{i,j}$ are the constituent concentrations in sublayer elements before and after this computation (when j=1, the wedge concentration C_i replaces the term $c'_{i,j-1}$) and C_S and c_{t_j} are the boundary conditions for the constituent concentration at the estuary mouth and at the wedge toe, respectively. (They are discussed in the section "Boundary Conditions.") The matrix U appearing in equation 11 is different for each of the three sublayers.

In those cases where $U_{i,10}$ and $U_{i,9}$ or $U_{i,11}$ are the only two nonzero terms in a row of the matrix U, this numerical scheme for modeling longitudinal advection is identical to the common explicit upstream finite-difference scheme. When there are other nonzero terms, the schemes are different, and the present scheme is stable while the common upstream difference scheme is not.

When water volumes from two or more elements combine in one element, as would occur in the example shown in figure 5, the inherent mixing of the volumes is numerical mixing in the longitudinal direction. The numerical scheme used for computing vertical advection similarly introduces numerical mixing in the vertical direction.

The boundary conditions for the constituent concentrations (the concentrations in the inflowing water) at the estuary mouth, C_S, are the same for the entire upper layer and the wedge. These boundary conditions are input data for the model.

Boundary conditions for constituent concentrations at the wedge toe are required only for the upper layer. The model computes these boundary conditions with the equation

$$c_{t_j} = \frac{C_1 Q'_{s_j} Q_s + c_f Q'_{f_j} Q_f}{Q'_{s_j} Q_s + Q'_{f_j} Q_f}, \qquad (12)$$

which determines the concentration of a mixture of (1) water from the wedge at the toe with a concentration of C_1 and (2) freshwater entering the upper layer at the toe with a concentration of c_f. The value of c_f for each constituent is input data for the model.

DIFFUSION

The final water-transport computation in a time step is for vertical turbulent diffusion between sublayers; there is no diffusion between the wedge and the upper layer in the model. To compute vertical transport by turbulent diffusion, the model uses a constant vertical diffusion coefficient, ϵ_y, in the equation,

$$c_{i,j} = c'_{i,j} + \frac{\epsilon_y \cdot \Delta t}{d_i^2} \left[(c'_{i,j-1} - c'_{i,j})_{j \neq 1} + (c'_{i,j+1} - c'_{i,j})_{j \neq 3} \right], \qquad (13)$$

where $c'_{i,j}$ and $c_{i,j}$ now represent constituent concentrations before and after this computation.

CONSTITUENT MODELS

GENERAL DESCRIPTION

This section describes processes, other than water transport, that affect the constituent concentrations. The constituents discussed are salinity, temperature (heat), chlorophyll *a* (phytoplankton), 5-day BOD, and DO. Although information on the DO concentrations is the goal of the computations, the concentrations of the other constituents must also be computed because they affect the DO concentrations.

SALINITY

Salt enters the estuary from the sea and is transported through the estuary by the processes already described. No other sources of salt are considered. The model computes salinities of the sublayer elements in the upper layer, but the salinity in the entire wedge is assumed to equal the salinity of the inflowing seawater. The model treats sea salt as a conservative substance; computations for chemical reactions or other processes are not necessary.

TEMPERATURE

The model computes the temperature of each of the elements in the upper layer, $T_{i,j}$, and also in the wedge, T_{w_i}. In addition to heat transfer by advection and diffusion within the estuary, heat transfer occurs between the top sublayer and the atmosphere, and all sublayers and the wedge are heated (though not equally) by solar radiation.

The program computes the heat transfer at the water surface by using the procedure given by Yotsukura, Jackman, and Faust (1973). The rate of heat transfer between the atmosphere and the water per unit area of water surface, H, is approximated by the linear expression,

$$H = H_S + H_L + H_b + (T_s - T_b)\frac{dH_b}{dT_b}, \qquad (14)$$

where

H_S = rate of solar energy penetrating a unit area of water surface;
H_L = rate of incoming long-wave radiation per unit area water surface;
H_b = heat transfer rate per unit area of water surface due to outgoing long-wave radiation, evaporation, and conduction when the water surface temperature is T_b;
T_b = a reference temperature; and
T_s = water surface temperature.

Positive values of these quantities denote heat transfer from the atmosphere to the water, and negative values denote heat transfer from the water to the atmosphere.

The program computes the quantities H_b and dH_b/dT_b once at the beginning of every day using daily average meteorological data and $T_b = T_{1,3}$. Meteorological data required by the model are

R_a = mean daily relative humidity, in percent;
S_R = total daily incident solar radiation, in gram-calories per square centimetre (g-cal/cm^2);
T_a = mean daily air temperature, in degrees Celsius; and
W_a = mean daily wind speed, in feet per second.

Also required is coefficient C_r, which is used to compute the incoming long-wave radiation.

The heat transfer rate H_b and its derivative are computed using the following equations, which were given by Yotsukura, Jackman, and Faust (1973):

$$H_b = -\left[\epsilon\sigma(T_b + \delta)^4\right] - \left[\lambda W_a(\alpha - \beta T_b)(E(T_b) - E_a)\right] - \left[\gamma\lambda P W_a(\alpha - \beta T_b)(T_b - T_a)\right] \qquad (15)$$

and

$$\frac{dH_b}{dT_b} = -4\epsilon\sigma(T_b+\delta)^3 - \lambda W_a \frac{dE(T_b)}{dT_b} - \alpha\lambda\gamma P W_a. \quad (16)$$

The three bracketed terms on the right side of equation 15 represent heat-transfer rates due to outgoing long-wave radiation, evaporation, and conduction, respectively. The variables appearing in equations 15 and 16 are defined as follows:

E_a = vapor pressure in air, in millibars;
$E(T_b)$ = saturation vapor pressure in air at temperature T_b, in millibars;
P = atmospheric pressure, assumed to be 1,013 millibars;
α = 595.9 g-cal/g, latent heat of vaporization at 0°C;
β = 0.545 g-cal·g^{-1}·°C^{-1}, change in latent heat of vaporization per unit change in temperature;
γ = 0.61×10^{-3}/°C, constant in the Bowen ratio relating heat transfer by conduction to evaporation;
δ = 273 K (kelvin), constant to convert degrees Celsius to kelvin units;
ϵ = 0.97, emissivity of water;
λ = 3.6×10^{-4} g·cm^{-2} hr^{-1}·mb^{-1} (ft/s)$^{-1}$, mass-transfer coefficient for evaporation; and
σ = 4.88×10^{-9} g-cal·cm^{-2}· hr^{-1}·K^{-1}, Stefan-Boltsman constant.

With the exception of λ the above coefficients were taken from Yotsukura, Jackman, and Faust (1973). The present value of λ is based on more recent work by H. E. Jobson (oral commun., 1974) and is about twice the value given by Yotsukura, Jackman, and Faust (1973).

The saturation vapor pressure at temperature T_b and its derivative are approximated with the expressions

$$E(T_b) = \xi\exp(\zeta - \frac{\eta}{T_b+\delta}) \quad (17)$$

and

$$\frac{dE(T_b)}{dT_b} = E(T_b)\frac{\eta}{(T_b+\delta)^2} \quad (18)$$

where ξ = 23.38 mbar; η= 5303.3 K; and ζ=18.1.

The model approximates heat transfer to the water by incoming long-wave radiation, H_L, by the following equation, proposed by Koberg (1964):

$$H_L = (C_r + 0.0263\sqrt{E_a})\sigma(T_a+\delta)^4. \quad (19)$$

The coefficient C_r is a function of the air temperature and the ratio of the actual to the clear-sky incident solar radiation. Koberg (1964) presents C_r in graphical form; it has a numerical value of the order 0.7.

The model computes the quantities H_L, H_b, and dH_b/dT_b for each day using mean-daily meteorological data and the values of $T_{1,3}$ at the start of the day for T_b. During each time step the temperature of each element in the top sublayer is changed according to the relation

$$T_{i,3} = T'_{i,3} + [H_L + H_b + (T'_{i,3} - T_b)(dH_b/dT_b)] \Delta t/(30.48\, d_i), \quad (20)$$

where $T'_{i,3}$ and $T_{i,3}$ are the temperatures of an element before and after this heat-transfer computation. The numerical constant in equation 20 converts the dimensions of the element thickness, d_i, from feet to centimetres.

The amount of solar radiation penetrating a unit area of water surface during a time step, H_s, is calculated with equation 21a or 21b,

$$H_s = S'_R S_R \frac{\pi}{N_t}\sin\theta,\ 0\leq\theta\leq\pi \quad (21a)$$

$$H_s = 0,\ \theta<0 \text{ or } \theta>\pi, \quad (21b)$$

where θ is the angle

$$\theta = 2\pi(I_t - \frac{N_t}{4} - \frac{1}{2})/N_t, \quad (22)$$

where l_t is the number of the time step; N_t is the total number of time steps in a day; and S'_R is the fraction of the incident solar radiation that penetrates the water surface.

The model computes the effect of solar heating on each sublayer element in the upper layer by taking the difference between the solar energy entering a unit area of the top, $H^*_{i,j+1}$, and leaving the bottom, $H^*_{i,j}$, of each element. These quantities are related by the equation

$$H^*_{i,j} = H^*_{i,j+1}\exp(-k_{i,j}d_i), \quad (23)$$

where $k_{i,j}$ is the solar-radiation attenuation coefficient for a sublayer element. Thus, during every time step the model changes the temperature of each sublayer element by the equation

$$T_{i,j} = T'_{i,j} + (H^*_{i,j+1} - H^*_{i,j})/(30.48\, d_i), \quad (24)$$

where $T'_{i,j}$ and $T_{i,j}$ are now the temperatures before and after a solar-heating calculation.

The model changes the temperatures of elements in

the wedge, T_{w_i}, according to equation 25, which was derived with the assumption that all solar energy passing through the wedge–upper layer interface heats the wedge elements:

$$T_{w_i} = T'_{w_i} + H^*_{i,1} B_i / (30.48\, A_i), \tag{25}$$

where T'_{w_i} and T_{w_i} are the temperatures before and after the solar-heating calculation.

PHYTOPLANKTON

In addition to calculating the transport of phytoplankton by advection and diffusion, the model considers the growth, respiration, and settling of the phytoplankton. In this report growth is defined as the increase in phytoplankton biomass by both reproduction and by the increase in size of the individual plankters. Respiration includes all those processes that cause a decrease in phytoplankton biomass and all those processes by which living and dead (decomposing) phytoplankton use oxygen. All phytoplankton are represented in the model as chlorophyll *a*. Chlorophyll *a* concentrations are denoted in the upper layer by $CP_{i,j}$, and in the wedge by CP_{w_i}. Because of insufficient data, no attempt is made to distinguish between different taxa, even though it is known that species of both freshwater and saltwater origin bloom in the estuary (see section "Supplemental Information" under "Phytoplankton"), and that the different species probably respond differently to changes in salinity, temperature, and other parameters.

Growth and respiration are modeled by adding the amount

$$\Delta CP_{i,j} = CP'_{i,j}\,(G-R)\Delta t \tag{26}$$

or

$$\Delta CP_{w_i} = CP'_{w_i}\,(G-R)\Delta t \tag{27}$$

to the chlorophyll *a* concentrations in the sublayer or the wedge elements, respectively. The quantities $CP'_{i,j}$ and CP'_{w_i} represent chlorophyll *a* concentrations before this addition. The variables R and G are respiration and growth rates. The respiration rate used by the model doubles with every 10°C rise in temperature (see for example McKee and Wolf, 1963, p. 284) and is given by

$$R = R_{20} \exp\left[0.0693(T-20)\right], \tag{28}$$

where R_{20} is R at 20°C and T is the local water temperature. The growth rate is a function of the local temperature and solar-radiation intensity,

$$G = F_T F_L\, G_o, \tag{29}$$

where G_o is the maximum growth rate and F_T and F_L are functions of temperature and solar-radiation intensity, respectively. The temperature function used by the model is

$$\begin{aligned} F_T &= 0, && (T<10°) \\ F_T &= 0.1\,T-1.0, && (10°\leq T\leq 20°) \\ F_T &= 1.0, && (T>20°). \end{aligned} \tag{30}$$

The solar-radiation function is

$$F_L = \frac{L}{L_o}\exp\left(1-\frac{L}{L_o}\right), \tag{31}$$

where L is the depth-averaged solar-radiation intensity in the wedge or sublayer element where the growth rate is desired and L_o is L for maximum growth. Both F_T and F_L are shown in figure 6.

Equation 30 is the authors' approximation of the effect of temperature on phytoplankton growth; it is based on data by Jitts, McAllister, Stephens, and Strickland (1964) for some marine phytoplankton and on knowledge that phytoplankton blooms are normally observed in the Duwamish estuary when the freshwater temperatures are about 20°C or higher.

Equation 31, which describes the effect of solar radiation on phytoplankton growth, was previously used by Steele (1962) for computing the effect of light on photosynthesis.

The model computes an average value of L for a sublayer element with the equation

$$L = \frac{H^*_{i,j+1}}{\Delta t}\,\frac{1-\exp(-k_{i,j}\,d_i)}{k_{i,j}\,d_i} \tag{32}$$

and for a wedge element with

$$L = \frac{H^*_{i,1}}{\Delta t}\,\frac{1-\exp(-k_{w_i}A_i/B_i)}{k_{w_i}\,A_i/B_i}, \tag{33}$$

where $k_{i,j}$ and k_{wi} are solar-radiation attenuation coefficients for the sublayer and wedge elements.

The attenuation coefficients for the sublayer and wedge elements are approximated by

$$k_{i,j} = k^o{}_u + k_C\, CP_{i,j} \tag{34}$$

and

$$k_{w_i} = k^o{}_w + k_C\, CP_{w_i}, \tag{35}$$

where $k^o{}_u$ and $k^o{}_w$ are the attenuation coefficients of the sublayers and the wedge in the absence of phytoplankton (chlorophyll *a*) and k_C is the increase in the attenu-

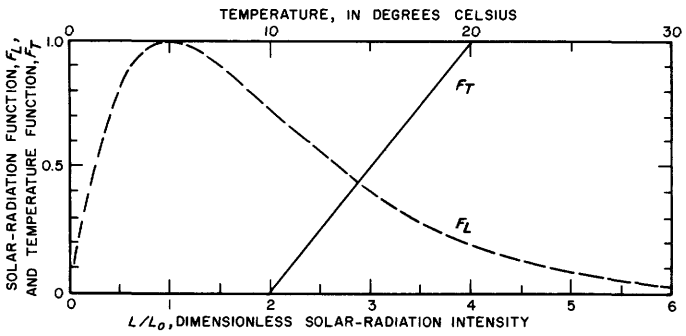

FIGURE 6.—Solar-radiation and temperature functions for computing phytoplankton growth rates.

ation coefficient due to a unit increase in chlorophyll *a* concentration.

The effects of nutrient concentrations on phytoplankton growth were not modeled in this study because present nutrient concentrations in the Duwamish River estuary are believed high enough, even during phytoplankton blooms, not to have an important effect on the growth rate. Data on phytoplankton in the estuary and a discussion of the probable effects of nutrients on phytoplankton growth rates in the estuary appear in the section "Estimated Influence of Nutrients on Phytoplankton Growth."

The net amount of oxygen produced in the upper layer by the phytoplankton through photosynthesis and respiration is assumed to be proportional to $\Delta CP_{i,j}$. (See equation 45.)

Because of settling of phytoplankton, the wedge receives chlorophyll *a* from the upper layer and loses chlorophyll *a* by deposition of phytoplankton on the channel bottom; resuspension from the bottom is not modeled. For every time step, the model performs the following settling computation for each wedge element, equation 36, and each sublayer element, equation 37:

$$CP_{w_i} = CP'_{w_i} + (CP'_{i,1} - CP'_{w_i})\mathrm{w}\,\Delta t\, B_i / A_i \quad (36)$$

and

$$CP_{i,j} = CP'_{i,j} + (CP'_{i,j+1} - CP'_{i,j})\, w\Delta t/d_i, \quad (37)$$

where CP'_{w_i} and CP_{w_i}, and $CP'_{i,j+1}$ and $CP_{i,j}$ are the chlorophyll *a* concentrations before and after the settling computation and w is a constant settling velocity.

BIOCHEMICAL OXYGEN DEMAND

The present model computes the BOD (5-day biochemical oxygen demand) in the upper layer of the estuary. BOD was not modeled in the wedge because the processes that transport BOD into the wedge are largely unknown. A constant BOD, equal to the BOD of the seawater, was assumed for the entire wedge. Data from the Duwamish River estuary (Welch, 1969) show that the BOD is typically 1–2 mg/l (milligrams per litre) and exceeds 5 mg/l only during phytoplankton blooms. The present low BOD has only a small effect on the dissolved oxygen in the upper layer of the estuary. However, because increased discharges from RTP probably will increase the BOD in the estuary, BOD is modeled for the upper layer. Only the carbonaceous oxygen demand was modeled because the time of travel from the RTP outfall to the mouth of the estuary is about 5 days. The nitrogenous oxygen demand, which was not modeled, becomes important only for longer periods.

The sources of BOD in the model are those coming into the estuary from the river, the sea, and miscellaneous sources such as small industrial or domestic sewage discharges within the estuary. The miscellaneous sources downstream from First Avenue South Bridge are combined and distributed uniformly along the lengths of the three most seaward elements of the top sublayer.

For every time step, the model performs the computation

$$\mathrm{BOD}_{i,3} = \mathrm{BOD}'_{i,3} + \mathrm{BOD}_M/(N_t\, 62.4\times 10^{-6} \sum_{n=i_{\max}-2}^{i_{\max}} V_{s_n}), \quad (38)$$

for $i = i_{\max} - 2$ to $i_{\max}$, where BOD_M is the miscellaneous BOD, in pounds per day, added to the estuary downstream from the First Avenue South Bridge; the numerical constant in equation 38 converts the units of the term in which it appears to milligrams per litre; and V_{s_n} is the volume of a sublayer element.

The BOD of the freshwater flow at the wedge toe, BOD_f, is computed within the model by the equation

$$\mathrm{BOD}_f = \frac{Q_R\,\mathrm{BOD}_R + Q_{\mathrm{RTP}}\,\mathrm{BOD}_{\mathrm{RTP}} + 0.185\,\mathrm{BOD}_T}{Q_R + Q_{\mathrm{RTP}}}. \quad (39)$$

The quantity BOD_f has units of milligrams per litre and is the BOD of a mixture of (1) the mean daily flow of the Green River at the Tukwila gage, Q_R, with a concentration of BOD_R; (2) the mean daily flow rate from RTP, Q_{RTP}, with a concentration of $\mathrm{BOD}_{\mathrm{RTP}}$; and (3) miscellaneous BOD inputs to the estuary upstream from First Avenue South Bridge, BOD_T, expressed in pounds of BOD per day.

The model treats the decay of BOD as a first-order reaction and computes the change in BOD due to decay

with the equation

$$\Delta BOD_{i,j} = -K_{BOD} BOD'_{i,j} \Delta t, \quad (40)$$

where $\Delta BOD_{i,j}$ is the change in BOD of an element due to decay during a time step and K_{BOD} is a temperature-dependent decay rate. The oxygen consumed by the BOD is assumed to be proportional to $\Delta BOD_{i,j}$. (See equation 45.)

The decay rate at 20°C, K^{20}_{BOD}, is data input to the model, and the decay rate at other temperatures is computed by the equation

$$K_{BOD} = K^{20}_{BOD} \exp\left[0.046(T-20°)\right], \quad (41)$$

which is derived from information given by Fair, Geyer, and Okun (1971, p. 645).

DISSOLVED OXYGEN

The processes in the model that affect the DO (dissolved-oxygen) concentrations are the exchange of oxygen between the water and the atmosphere, commonly called atmospheric reaeration; the production and consumption of oxygen by phytoplankton; and the consumption of oxygen by BOD. These processes are modeled explicitly only in the upper layer. DO in the wedge is modeled by using an oxygen-consumption rate as was done by Stoner, Haushild, and McConnell (1974).

The effect of reaeration is computed—only for the top sublayer—by the linear equation

$$DO_{i,3} = DO'_{i,3} + r\,(DO^s_{i,3} - DO'_{i,3})\,\Delta t, \quad (42)$$

where the quantities $DO'_{i,3}$ and $DO_{i,3}$ are DO concentrations of elements in the top sublayer before and after the reaeration computation; r is a temperature-dependent reaeration coefficient; and $DO^s_{i,3}$ is the saturation concentration of the top sublayer element in segment i. The DO saturation concentration is computed by the equation

$$DO^s_{i,3} = (487 - 2.65S_{i,3})/(33.5 + T_{i,3}), \quad (43)$$

where $S_{i,j}$ is the salinity in parts per thousand and $T_{i,j}$ is the temperature, in degrees Celsius, of sublayer element i,j. The equation was taken from a report by the Thames Survey Committee and the Water Pollution Research Laboratory (1964, p. 349), but one coefficient was changed to give a better fit to the data of G. C. Whipple and M. C. Whipple (American Public Health Association and others, 1971, p. 480).

The model computes the reaeration coefficient, r, by the equation

$$r = (5|v_i|/d_i^{5/3}) \exp\left[0.024(T_{i,3}-20)\right], \quad (44)$$

where v_i is the velocity of the water in the top sublayer relative to the velocity of that in the wedge. The dimension of r in the equation is days $^{-1}$ when v_i is in feet per second and d_i is in feet. The first term in parentheses is an adaptation of an equation for the reaeration coefficient in homogeneous streams by M. A. Churchill, H. L. Elmore, and R. A. Buckingham, and the exponential function is a temperature correction made by H. G. Becker; both are reported by Fair, Geyer, and Okun (1971, p. 651).

To account for the effects of BOD and phytoplankton, the model changes the DO concentrations of sublayer elements according to the equation

$$DO_{i,j} = DO'_{i,j} + DO_C\,\Delta CP_{i,j} + DO_{BOD}\,\Delta BOD_{i,j}, \quad (45)$$

where the differences $\Delta CP_{i,j}$ and $\Delta BOD_{i,j}$ are given by equations 26 and 40, respectively, and the coefficients DO_C and DO_{BOD} are the changes in DO concentration associated with unit changes in chlorophyll a concentration and BOD.

The DO concentration of each wedge element, DO_{w_i}, is changed for every time step by the equation

$$DO_{w_i} = DO'_{w_i} - \Delta DO_w \Delta t, \quad (46)$$

where ΔDO_w is a rate of oxygen consumption in the wedge, which includes the effects of all dissolved-, suspended-, and benthic-oxygen demands.

APPLICATION OF THE MODEL TO THE DUWAMISH RIVER ESTUARY

GENERAL

Computations for the model of the Duwamish River estuary were made using historical input data for parts of the periods June–September 1967–69 and 1971. A second set of computations was made using most of the input data for 1971 and increasing the effluent discharge from RTP to the maximum magnitude expected in the future.

Parameters in the model that could be varied were adjusted to give the best agreement between computed and observed data for the 1968 period. These parameters were not changed for the other years.

INPUT DATA

FLOW MODEL

The items required by the model for computing flow in the estuary are listed in table 1. Values or equations for some items are given either in this table or in tables 2 and 3. The estuary geometry, wedge-toe location, tide stages, tidal-prism thickness, upper-layer thickness at mouth, slope of upper layer-wedge interface, and freshwater inflow are identical to those used by Stoner, Haushild, and McConnell (1974). Data for the cross

TABLE 1.—*Data required for computing flow in the Duwamish River estuary*

Item	Value
Geometry of the estuary	See table 2.
Location of wedge toe	See table 3.
Tide stage	See section "Input Data," paragraph 2.
Tidal-prism thickness (ft)	P_t; see section "Input Data," paragraph 2.
Thickness of upper layer at mouth (ft)	$D=2.5+0.3P_t+0.003Q_f$.
Slope of upper layer-wedge interface (ft/ft)	$S_o=0.00006$.
Freshwater inflow at head of estuary (ft^3/s)	Q_f, see section "Input Data," paragraph 3.
Distribution of freshwater inflow among sublayers	$Q'_{f_j}=0.1, 0.4, 0.5 (j=1, 2, 3)$.
Average rate of transport of saltwater upstream from wedge toe (ft^3/s)	$Q_s=200$.
Distribution of saltwater inflow among sublayers	$Q'_{s_j}=0.65, 0.20, 0.15 (j=1, 2, 3)$.
Entrainment velocity across upper layer-wedge interface (ft/s)	$U_e=-6.5\times10^{-7}+3.25\times10^{-6}P_t+4.5\times10^{-8}Q_f$.
Dimensions vertical velocities at base of sublayers	$U'_{e_j}=1.0, 0.8, 0.5 (j=1, 2, 3)$.
Vertical diffusion coefficient (ft^2/s)	$\epsilon_y=0.0001$.

TABLE 2.—*Relation of width to elevation at cross sections for computing geometry of the Duwamish River estuary*

[Elevations are in feet above mean lower low water, and widths are in feet. The mouth is defined as 3,500 ft downstream from the Spokane Street Bridge.]

Cross-section 1, at mouth:[1]					
Elevation	−31	−20	−9	2	15
Width	175	302	378	476	640
Cross-section 2, 2,000 feet upstream from mouth:					
Elevation	−31	−20	−9	2	15
Width	175	302	378	476	640
Cross-section 3, 4,000 feet upstream from estuary mouth:					
Elevation	−34	−22	−10	2	15
Width	50	319	485	590	706
Cross-section 4, 5,300 feet upstream from estuary mouth:					
Elevation	−49	−33	−17	−3	15
Width	11	640	984	1,068	1,148
Cross-section 5, 9,900 feet upstream from estuary mouth:					
Elevation	−31	−20	−9	2	15
Width	304	425	528	642	700
Cross-section 6, 14,700 feet upstream from estuary mouth:					
Elevation	−30	−19	−8	3	15
Width	153	229	274	358	500
Cross-section 7, 19,000 feet upstream from estuary mouth:					
Elevation	−19	−8	−1	6	15
Width	128	368	435	506	587
Cross-section 8, 24,700 feet upstream from estuary mouth:					
Elevation	−19	−8	−1	6	15
Width	223	281	346	427	500
Cross-section 9, 28,700 feet upstream from estuary mouth:					
Elevation	−12	−2	4	10	15
Width	478	572	622	668	690
Cross-section 10, 31,100 feet upstream from estuary mouth:					
Elevation	−11	−2	3	8	15
Width	229	242	252	267	280
Cross-section 11, 38,200 feet upstream from estuary mouth:					
Elevation	−10	−1	4	9	15
Width	120	141	162	183	200

[1]For modeling, this cross section was assumed the same as cross-section 2.

TABLE 3.—*Equations for computing location of wedge toe in Duwamish River estuary*

[Equations were fit to data collected mostly when Q_f was between 200 and 600 ft^3/s, with some data between 600 and 1,100 ft^3/s]

x_t = longitudinal coordinate of wedge toe, in feet upstream from estuary mouth.
Y = tide stage, in feet above mean lower low water.
Q_f = mean daily freshwater discharge, in cubic feet per second.
$X_1 = 25{,}151+1{,}626\,Y-79.95\,Y^2$
$X_2 = 22{,}188+1{,}210\,Y-36.10\,Y^2$
$X_3 = 21{,}276+768\,Y+0.60\,Y^2$
$X_4 = 20{,}400+638\,Y$
$X_5 = 20{,}200+526\,Y$

$x_t=19400$,	$Y<-1.6$,
$x_t=X_1$,	$Y\geq-1.6$, $Q_f\leq200$
$x_t=X_1-\frac{X_1-X_2}{200}(Q_f-200)$,	$Y\geq-1.6$, $200<Q_f<400$
$x_t=X_2-\frac{X_2-X_3}{200}(Q_f-400)$,	$Y\geq-1.6$, $400\leq Q_f<600$
$x_t=X_3-\frac{X_3-X_4}{500}(Q_f-600)$,	$Y\geq-1.6$, $600\leq Q_f<1100$
$x_t=X_4-\frac{X_4-X_5}{900}(Q_f-1100)$,	$Y\geq-1.6$, $1100\leq Q_f<2000$
$x_t=X_5$,	$Q_f\geq2000$

sections were obtained from 1971 maps by the U.S. Army Corps of Engineers of the dredged part of the estuary and from measurements by the U.S. Geological Survey of cross sections upstream from the dredged channel. The slope of the interface and the equations used to compute the location of the wedge toe and the thickness of the upper layer at the mouth were determined from observed data for the Duwamish River estuary. The errors in the upper layer thickness and wedge-toe location computed with the equations and the error in the interface slope probably average less than 25 percent.

Tide stages at hourly intervals are input data for the model; they are computed using the data for Seattle, Wash., and the procedures published by the [U.S.] Environmental Science Services Administration (1967–71). The model computes the tide stage at each time step by linear interpolation between the hourly stages. The tidal-prism thickness, P_t, is used by the model to compute the upper layer thickness at the mouth and the entrainment velocity across the upper layer-wedge interface. P_t is defined here as the difference between the sum of the two daily high and the sum of the two daily low tide stages.

The mean daily freshwater inflow to the estuary, Q_f, is the sum of the mean daily flow of the Green River at the Tukwila gaging station and the mean daily outflow from RTP, which was obtained from Metro records. Other freshwater inflows, such as that from the relic Black River, are negligibly small.

The values of the other required parameters, Q'_{fj}, Q_s, Q'_{sj}, U_e, U'_{ej}, and ϵ_y given in table 1 were determined by trial and error. They were varied, within some logical limits, until computed salinities agreed with observed salinities for the three sublayers at 16th Avenue South, First Avenue South, and Spokane Street Bridges. In order to improve the agreement between computed and observed salinities at Spokane Street Bridge, the values of some of these parameters differ a little from those used by Stoner, Haushild, and McConnell (1974). These investigators did not verify model salinities with the data from Spokane Street Bridge because calculations of advective transport in the upper layer near the estuary mouth sometimes were unstable in the model they used. In general, the agreement between the computed and observed salinities at 16th Avenue South and First Avenue South Bridges is equal for the present and the earlier reported values of these parameters.

The values of U_e computed by the equation in table 1 are 25 percent higher than comparable values used by Stoner, Haushild, and McConnell (1974); the dimensionless quantities, Q'_{fj}, Q'_{sj}, and U'_{ej}, also differ by about 25 percent. Vertical diffusion was not in the earlier model but was used in the present model to increase the computed salinities in the top sublayer near the mouth without further changing the flow rate there. A value for the vertical turbulent diffusion coefficient, ϵ_y, was estimated by computing the average depth value for a homogeneous density flow (Jobson and Sayre, 1970) with a depth and velocity typical of the upper layer in the Duwamish River estuary and multiplying this value by about 0.01 to account for the stabilizing effect of the density stratification in the estuary. The reducing factor could only be estimated within one order of magnitude by extrapolating data summarized by Nelson (1972).

CONSTITUENT MODELS

BOUNDARY CONDITIONS

The modeling of each constituent requires that the concentrations in the water flowing into the estuary at its mouth and at the toe of the wedge be known. These concentrations, called boundary conditions, are necessary input to the model and were determined from data for estuary water sampled by project personnel or automatic monitors at the locations shown in figure 1. The monitors, presently (1975) operated by Metro, record the conductivity, temperature, DO concentration, and other data at 6- to 12-minute intervals.

In the model, the boundary condition is the same for the wedge and the entire upper layer at the estuary mouth. Constituent concentrations there were usually determined from the data for water sampled near the bottom at Spokane Street Bridge.

Boundary conditions at the wedge toe are required for only the upper layer. They are computed in the model by equation 12, which requires freshwater concentrations, c_f, as input data to the model. Because transport and other processes act on the brackish water upstream from the wedge toe, it is seldom correct to equate c_f to the concentration observed in the freshwater part of the river. In this study, values of c_f for temperature, DO, and chlorophyll *a* were calculated by using data collected in the vicinity of the wedge toe in the equation

$$c_f = \frac{c_t\,(Q'_s\,Q_s + Q'_f Q_f) - C_1 Q'_s Q_s.}{Q'_f Q_f} \qquad (47)$$

This equation was derived by solving equation 12 for c_f and deleting the j subscripts. The concentration c_t in equation 47 is the constituent concentration at the 3-ft (1-m) depth at the computed location of the wedge toe and was determined by interpolation between observed concentrations for the same depth at 16th Avenue South Bridge and East Marginal Way Bridge, and occasionally at Boeing Bridge. The observed concentration near the bottom at 16th Avenue South Bridge was substituted for C_1. Values of Q'_s and Q'_f for the 3-ft (1-m) depth were estimated by interpolation in the vertical direction between the centers of the sublayers.

Thus, except for salinity or for some other conservative constituents with slowly varying or steady concentrations for which there are no sources in the reach between the freshwater part of the river and the wedge toe, the concentrations c_f are not necessarily the concentrations in the true freshwater inflow. The concentrations c_f are artificial concentrations computed from available observed concentrations so that when they are used in equation 12, the computed sublayer concentrations at the wedge toe, c_{tj}, approximate the observed concentrations there. Changes in concentrations in the brackish waters between the end of freshwater flow and the toe are incorporated in the definition of c_f.

SALINITY

The only additional input data needed to model salinity are the salinities of the seawater and the river water. In the Duwamish River estuary they are 25 and 0 ppt, respectively.

TEMPERATURE

Input data required by the temperature model are the temperatures of the seawater and of the freshwater inflow to the estuary, and the meteorological data that is used to compute heat transfer at the water surface.

The temperature of the sea is taken as the daily minimum temperature measured by the bottom monitor at Spokane Street Bridge. The temperature of the freshwater is hourly input data. These are computed—by the method described earlier—from data from the surface monitors at the 16th Avenue South and East Marginal Way Bridges.

The meteorological data required by the model are the total incident solar radiation for the day and the mean daily values of air temperature, wind speed, relative humidity, and a coefficient for computing incident long-wave radiation. These data were determined from information collected at the Seattle-Tacoma International Airport by the [U.S.] Environmental Science Services Administration (1967–69) and the [U.S.] National Oceanic and Atmospheric Administration (1971). The coefficient for computing incident long-wave radiation was calculated using the information given by Koberg (1964) and the other meteorological data.

PHYTOPLANKTON

The data required by the phytoplankton model, which computes chlorophyll *a* concentrations, are listed in table 4. The chlorophyll *a* concentration in the seawater is typical of what was found in samples from Elliott Bay. The chlorophyll *a* concentrations of the freshwater are daily input data for the model. These concentrations were calculated using equation 47 and data for water sampled from the 3-ft (1-m) depth at 16th Avenue South, Boeing, and East Marginal Way Bridges, and from near the bottom at 16th Avenue South Bridge. Data are available for samples collected twice daily about two times a week during the years 1967–69. Although hourly data are preferred, the data were sufficient only to estimate daily values of CP_f.

Usually, data were not available to evaluate directly many of the remaining parameters required in the phytoplankton model. Values in table 4 often were selected because they gave the best agreements between the computed and observed chlorophyll *a* and DO concentrations for the summer of 1968. No systematic attempt was made to determine the combination of parameters that give a statistically best agreement between computed and observed data; instead, decisions were made by visually comparing the plotted data. Attempts were always made to select values of the parameters within the range of those published in reports on research of the individual phenomena or in other reports on ecosystem models (for example, DiToro and others, 1971; or Chen and Orlob, 1972).

The phytoplankton settling velocity was chosen so that computed chlorophyll *a* concentrations agreed with observed concentrations in the wedge. The tabulated value is at the lower end of the range of the values reported by Hutchinson (1967, p. 277) for marine diatoms.

TABLE 4.—*Data required for the phytoplankton model*

Item	Symbol	Value
Chlorophyll *a* concentration of seawater	CP_S	1 μg/l
Chlorophyll *a* concentration of freshwater inflow at toe	CP_f	Variable
Phytoplankton settling velocity	w	0.00002 ft/s
Solar-radiation-attenuation coefficient in upper layer in the absence of phytoplankton (chlorophyll *a*)	k_u^o	0.25 ft^{-1}
Solar-radiation-attenuation coefficient in wedge in the absence of phytoplankton (chlorophyll *a*)	k_w^o	0.125 ft^{-1}
Change in solar radiation-attenuation coefficient due to a unit change in chlorophyll *a* concentration	k_C	0.005 $ft^{-1}/(\mu g$ chlorophyll *a*/l)
Maximum growth rate of phytoplankton	G_o	0.2 hr^{-1}
Solar-radiation intensity for maximum phytoplankton growth	L_o	10 g-cal·cm^{-2}·hr^{-1}
Respiration rate at 20°C	R_{20}	0.004 hr^{-1}
Oxygen produced during growth or consumed during respiration for a unit change in chlorophyll *a* concentration	DO_C	0.125 mgO_2/μg chlorophyll *a*

The solar-radiation attenuation coefficient in the absence of phytoplankton in the upper layer, $k^o{}_u$, was estimated, by using a few Secchi-disc depths in equation 48, which was suggested by Poole and Atkins (see Sverdrup and others, 1961, p. 92). The Secchi-disc depths averaged about 6 ft (2 m) and were obtained during periods of low chlorophyll *a* concentrations:

$$k^o{}_u = \frac{1.7}{\text{Secchi-disc depth}}. \qquad (48)$$

The constant of 0.73 in place of 1.7 in this equation as given by Welch (1969, p. 15) was not used because the computed solar-radiation intensity at a depth of 10 ft (3 m) would be one-third the intensity at the surface. According to D. L. Todd of Metro, who scuba dives in the Duwamish River estuary, the light intensity seems much less at that depth (oral commun., Nov. 1973). Furthermore, if one used 0.73 in equation 48, the computed bottom of the photic zone (estimated by Ryther, 1963, as the depth where the solar-radiation intensity is 1 percent of the intensity at the surface) would be about 40 ft (12 m). However, according to Welch (1969, p. 7), the photic zone is about 12 ft (4 m) deep.

Because Todd also noted that the water in the wedge was usually clearer than the water in the upper layer, the attenuation coefficient of the wedge in the absence

of chlorophyll a was selected arbitrarily to be one-half the value used in the upper layer.

Data from the Duwamish River estuary were not available to estimate the increase in the attenuation coefficient due to the presence of phytoplankton. The chosen value of k_C is an estimate based on data given by Megard (1973), Platt (1969), Ryther (1963), and Ryther and Yentsch (1957).

A maximum growth rate of 0.2 hr^{-1} used in the model gave the best agreement between computed and observed chlorophyll a concentrations in the upper layer. This value is about twice the maximum value computed with data from Jitts, McAlister, Stephans, and Strickland (1964) after adjusting their data for the length of their light and dark cycles. A growth rate of 0.2 hr^{-1} is equivalent to about 3.5 doublings per 12-hour day, which is a little greater than the usual range of 1 to 3 doublings per day (Talling, 1962, p. 744).

The solar-radiation (light) intensity for maximum growth, L_o = 10 g-cal·cm^{-2}·hr^{-1}, was selected so that maximum growth rates would occur during the clear summer days of the bloom periods. The computed daily average growth rate is a maximum at 3-ft (1-m) depth when the total daily solar radiation is 500 g-cal/cm^2 and the chlorophyll a concentration is about 45 μg/l (micrograms per litre). Jitts, McAlister, Stephans, and Strickland (1964) found that the optimum light intensity for cell division varied for different species and ranged from 4.5 to 18 g-cal·cm^{-2}·hr^{-1}. Strickland (1960, p. 11) reports that the optimum light intensity for photosynthesis is probably between 6 and 9 g-cal·cm^{-2}·hr^{-1}. However, data by Ryther (1956) shows that optimum light intensities ranged from about 1 to 4 g-cal·cm^{-2}·hr^{-1}.

The respiration rate, R, was calculated by using an oxygen-use rate during respiration of 3.5 ml (millilitres) oxygen per hour per gram dry weight of phytoplankton (estimated from data in Gibbs, 1962, p. 64), a mass density of oxygen at 1.43 g/l (grams per litre), a phytoplankton dry weight-to-chlorophyll a ratio of 100 (estimated from data in Strickland, 1960), and the tabulated value of DO_C=0.125 mg (milligrams) oxygen per microgram chlorophyll a (obtained by the procedure described in the section "Production and Consumption of Oxygen by Phytoplankton." The data yield

$$R=3.5\left(\frac{\text{ml } O_2}{\text{g dry weight/hour}}\right)\left(\frac{1.43\text{ g}}{1}\right)\left(\frac{100\text{ g dry weight}}{\text{g chlorophyll } a}\right)\left(\frac{\mu\text{g chlorophyll } a}{0.125\text{ mg } O_2}\right)=0.004/\text{hr}.$$

At maximum growth, the computed oxygen-production rate by photosynthesis is G_o DO_C = 0.025 mg oxygen per microgram chlorophyll a per hour. Data by Verduin (1956) yields 0.0064 mg oxygen per microgram chlorophyll a per hour. For a photosynthetic quotient (moles of CO_2/moles of O_2) equal to 1.2, the computed maximum production rate of carbon is 8 grams carbon per gram chlorophyll a per hour. Barlow, Lorenzen, and Myren (1963) report values between 8.7 and 16.3 grams carbon per gram chlorophyll a per hour for a eutrophic estuary. However, both Welch (1969, p. 17) and Shimada (1958) report values of the order 4 grams carbon per gram chlorophyll a per hour.

BIOCHEMICAL OXYGEN DEMAND

Data required by the BOD model are listed in tables 5 and 6. The values for BOD_S and BOD_R were based on observed data. Mean daily values for the BOD of the RTP effluent were determined from plant records. The BOD added to the estuary by miscellaneous discharges (table 6) was estimated from data furnished by Metro (Cecil Whitmore, written and oral communs., 1973).

The decay rate, K^{20}_{BOD}=0.25 day^{-1}, was calculated with data obtained from laboratory analyses of RTP effluent by Metro (R.I. Matsuda, written commun., 1973). The amount of oxygen consumed during the decay of a unit amount of BOD, DO_{BOD}=1.4, is related to the decay rate through the definitions of a first-order reaction and the 5-day BOD. The relationship is

TABLE 5.—*Data for the BOD model*

Item	Symbol	Value
BOD of seawater	BOD_S	1 mg/l
BOD of Green River at Tukwila gage	BOD_R	1 mg/l
Mean daily BOD of RTP effluent	BOD_{RTP}	Variable
Miscellaneous BOD added to estuary upstream of First Avenue South Bridge	BOD_T	See table 6
Miscellaneous BOD added to estuary downstream of First Avenue South Bridge	BOD_M	See table 6
BOD decay rate	K^{20}_{BOD}	0.25 day^{-1}
Oxygen consumed per unit decay of BOD	DO_{BOD}	1.4

TABLE 6.—*Miscellaneous BOD inflows to the Duwamish River estuary from upstream, BOD_T, and downstream, BOD_M, from First Avenue South Bridge*

[BOD is in pounds per day]

Year	BOD_T	BOD_M
1967	2,757	6,685
1968	824	6,685
1969	762	6,400
1971	762	0

$$DO_{BOD} = [1 - \exp(-5\,K^{20}_{BOD})]^{-1}. \quad (49)$$

DISSOLVED OXYGEN

A list of the data required by the DO model appears in table 7. Both the DO concentrations of the saltwater, DO_S, and of the freshwater, DO_f, are hourly inputs to the model. DO_S is set equal to the concentration measured by the bottom monitor at Spokane Street Bridge, and DO_f is computed using equation 47 and data from the surface monitors at 16th Avenue South and East Marginal Way Bridges and the bottom monitor at 16th Avenue South Bridge.

The rate of oxygen consumption in the wedge, ΔDO_w, is 25 percent greater than that reported by Stoner, Haushild, and McConnell (1974). The larger value was used because the entrainment velocity is higher and the residence time of water in the wedge is shorter in the present model than in the original model.

The method of selecting DO_{BOD} was described in the preceding section, and the procedure for estimating DO_C is described in the section "Production and Consumption of Oxygen by Phytoplankton."

MODEL VERIFICATION

GENERAL REMARKS

Constituent concentrations for the Duwamish River estuary were computed by the model for most of the June-September periods of 1967, 1969, and 1971 and for most of the June-August period of 1968. In figures 7–23, the computed temperatures, DO concentrations, and chlorophyll *a* concentrations in the upper layer for parts of these periods are compared with the appropriate observed data. The figures are grouped chronologically. Tide stages are plotted on the same figures as the temperature data.

No chlorophyll *a* data were available for 1971; therefore, the chlorophyll *a* concentration in the inflowing freshwater was assumed to be 1 μg/l. As a consequence,

TABLE 7.—*Data required for the DO model*

Item	Symbol	Value	Year
DO concentration of seawater	DO_S	Variable	----
DO concentration of freshwater inflow at toe	DO_f	Variable	----
Oxygen consumed per unit decay of BOD	DO_{BOD}	1.4	----
Oxygen produced or consumed during the growth or respiration of phytoplankton	DO_C	0.125 mg O_2/μg chlorophyll *a*	----
Oxygen consumption in wedge	ΔDO_w	0.035 (mg/l)/hr	1967
		0.029 (mg/l)/hr	1968
		0.033 (mg/l)/hr	1969
		0.020 (mg/l)/hr	1971

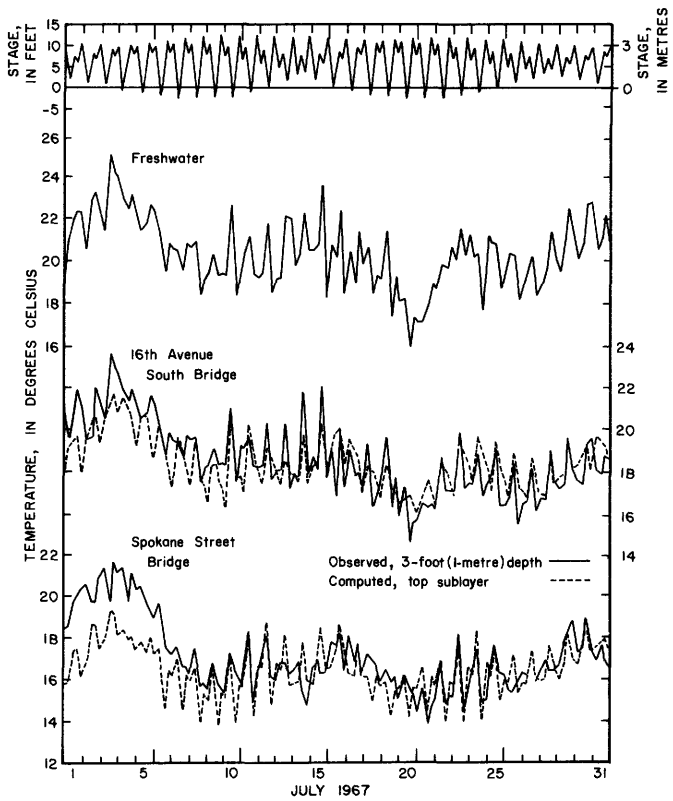

FIGURE 7.—Water temperatures and tide stages in Duwamish River estuary at times of high and low tides during July 1967.

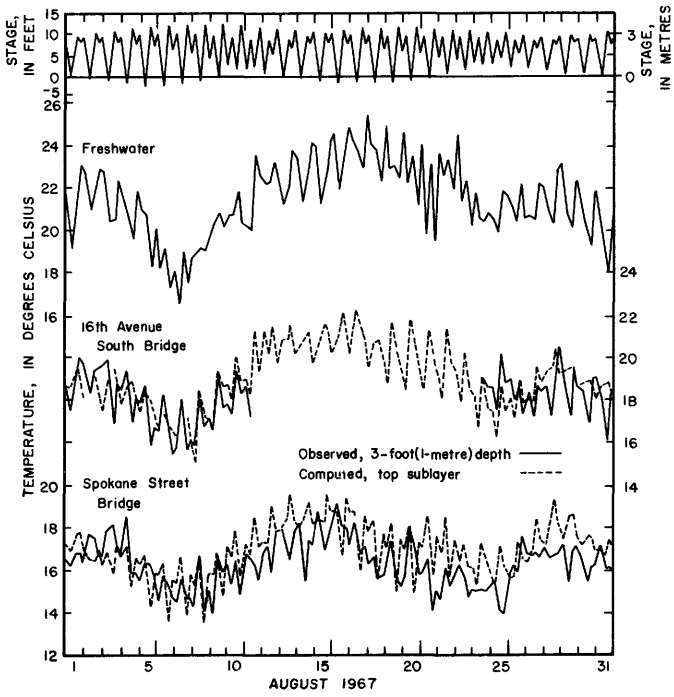

FIGURE 8.—Water temperatures and tide stages in Duwamish River estuary at times of high and low tides during August 1967.

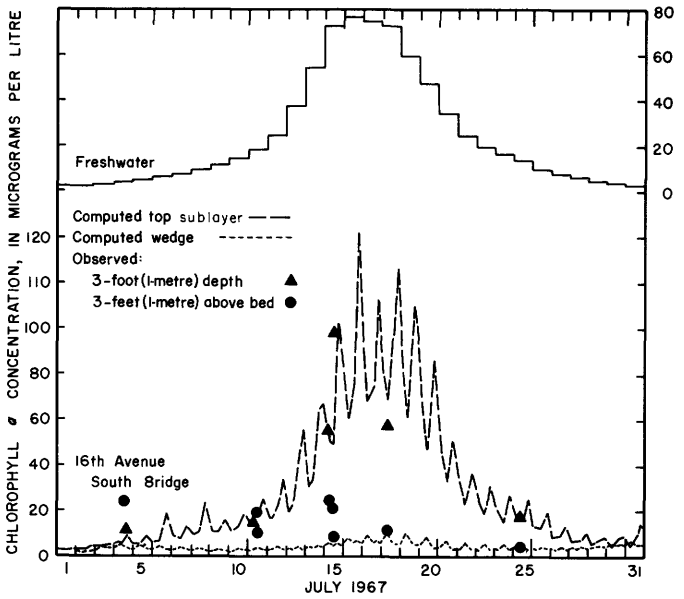

FIGURE 9.—Chlorophyll *a* concentrations in Duwamish River estuary at 16th Avenue South Bridge computed at times of high and low tides and observed about twice a day two times per week during July 1967.

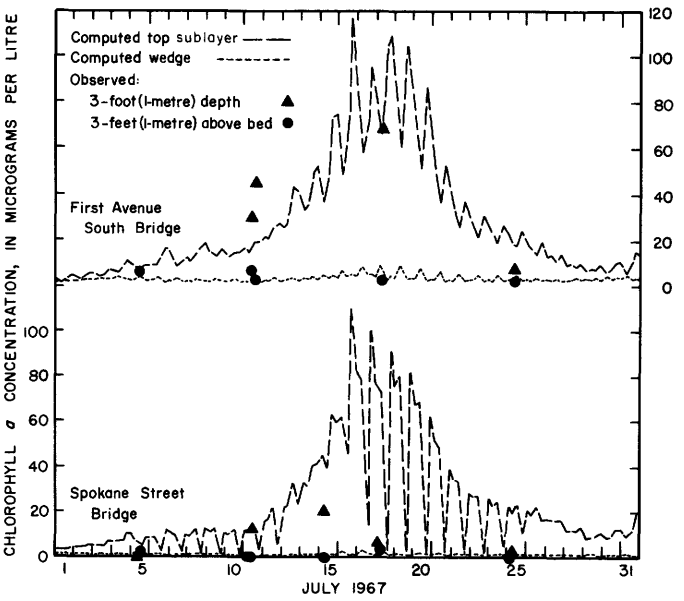

FIGURE 10.—Chlorophyll *a* concentrations in Duwamish River estuary at First Avenue South and Spokane Street Bridges computed at times of high and low tides and observed about twice a day two times per week during July 1967.

the computed phytoplankton (chlorophyll *a*) concentrations were sufficiently low so that neither photosynthesis nor respiration affected the computed DO concentrations. Although comparisons are not shown, the generally good agreements between computed and observed salinities were about the same as those of

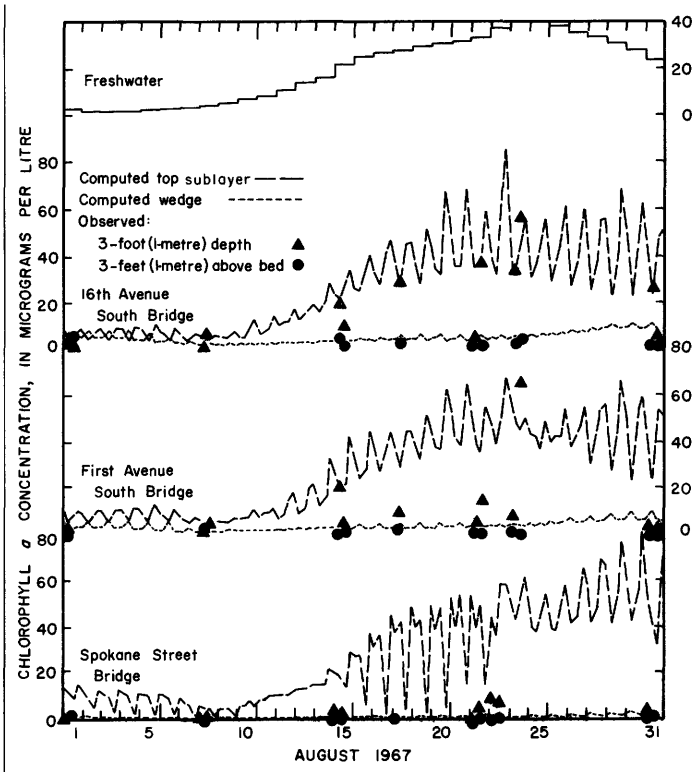

FIGURE 11.—Chlorophyll *a* concentrations in Duwamish River estuary computed at times of high and low tides and observed about twice a day two times per week during August 1967.

Stoner, Haushild, and McConnell (1974). Data for BOD also are not shown; the computed and observed BOD values were always low (about 2 mg/l or less). The low BOD had only a small effect on the computed DO concentrations.

For each period, graphs show the constituent concentrations in the freshwater inflow, which are input data, and the observed and computed concentrations at 16th Avenue South and Spokane Street Bridges. Chlorophyll *a* concentrations at First Avenue South Bridge also are given. Although the model can supply output concentrations for every 15 minutes, all graphs were drawn through data plotted only for each high and low tide. At some low tides, the upstream end of the model (wedge toe) was downstream from 16th Avenue South Bridge. For these times, the computed concentrations at the wedge toe were plotted in place of the computed data at 16th Avenue South Bridge. The observed temperature and DO-concentration data are from the automatic monitors that sample water from about the 3-ft (1-m) depth; the chlorophyll *a* data are from samples taken from a similar depth and from near the streambed. All computed data are for top-sublayer elements which almost always contain the observed data-collection points near the water surface.

Because 16th Avenue South Bridge is in the vicinity

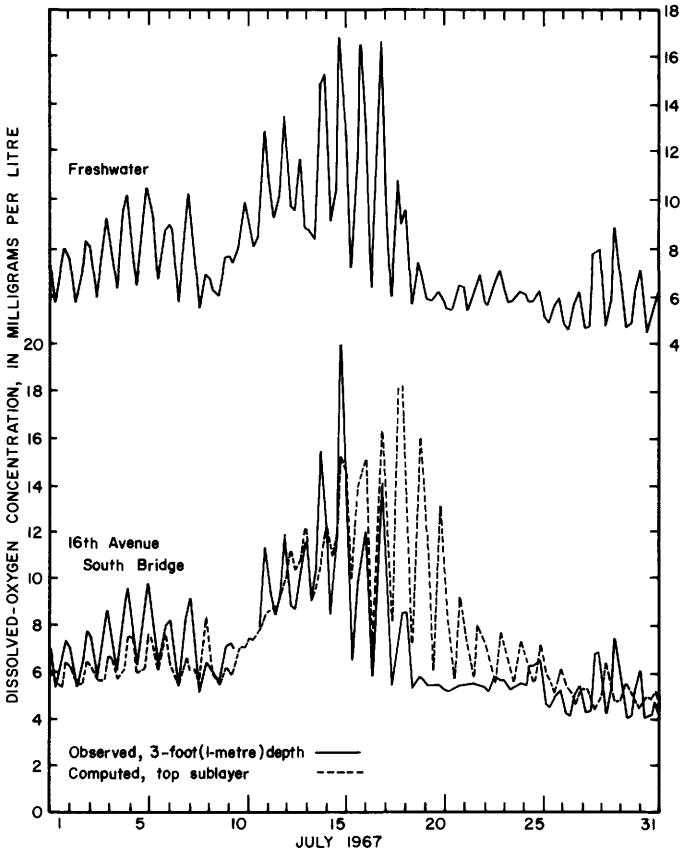

FIGURE 12.—Dissolved-oxygen concentrations in Duwamish River estuary at 16th Avenue South Bridge at times of high and low tides during July 1967.

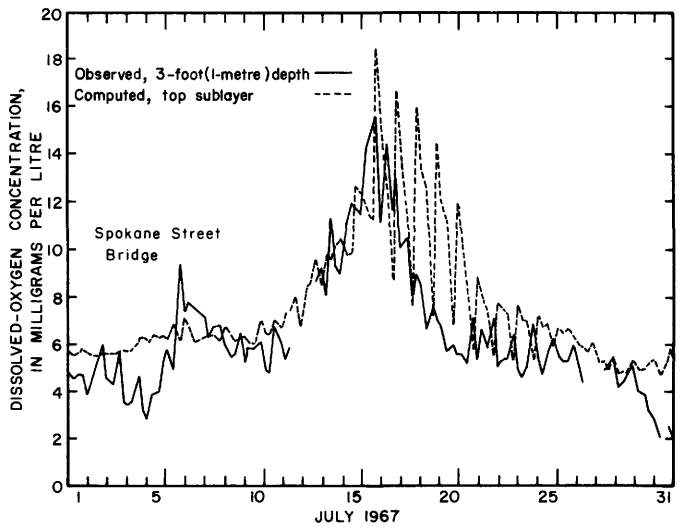

FIGURE 13.—Dissolved oxygen concentrations in Duwamish River estuary at Spokane Street Bridge at times of high and low tides during July 1967.

of the wedge toe, the differences between the observed and computed data at that station are measures of the

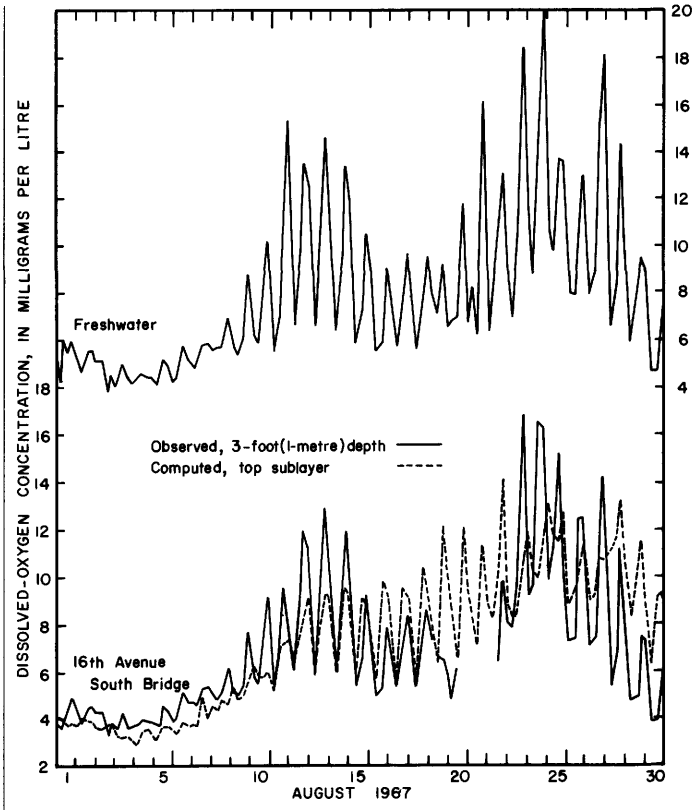

FIGURE 14.—Dissolved oxygen concentrations in Duwamish River estuary at 16th Avenue South Bridge at times of high and low tides during August 1967.

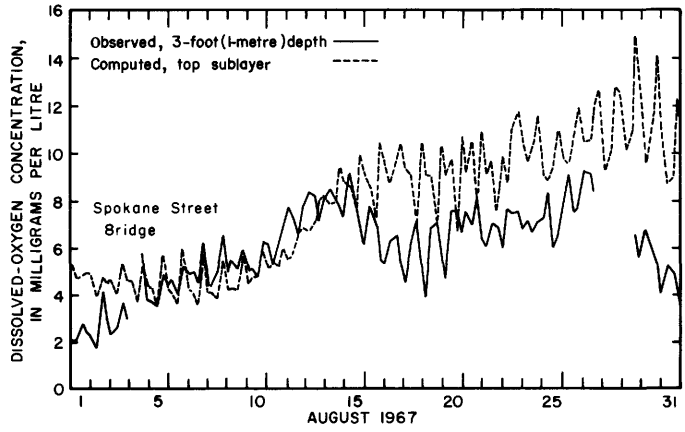

FIGURE 15.—Dissolved oxygen concentrations in Duwamish River estuary at Spokane Street Bridge at times of high and low tides during August 1967.

errors in the boundary conditions at the wedge toe. The differences between the observed and computed data at Spokane Street Bridge at low tide are measures of the errors of the upper layer models. The concentrations at Spokane Street Bridge at high tide are strongly dependent on the concentrations in Elliott Bay.

In each graph, the concentrations at 16th Avenue

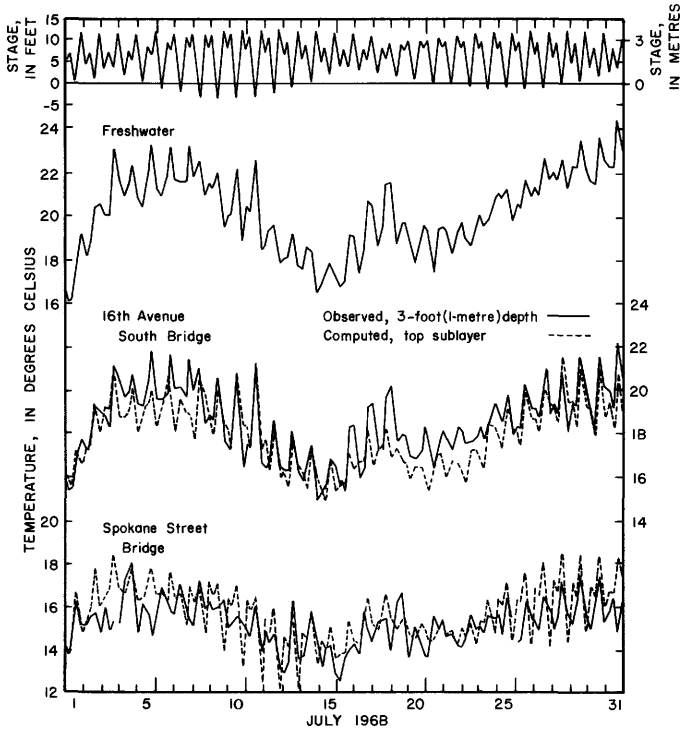

FIGURE 16.—Water temperatures and tide stages in Duwamish River estuary at times of high and low tides during July 1968.

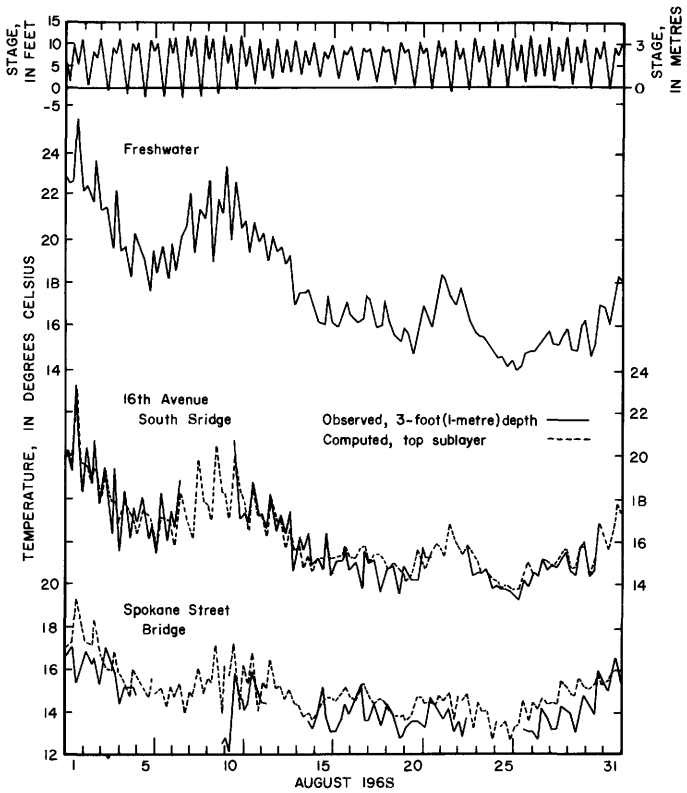

FIGURE 17.—Water temperatures and tide stages in Duwamish River estuary at times of high and low tides during August 1968.

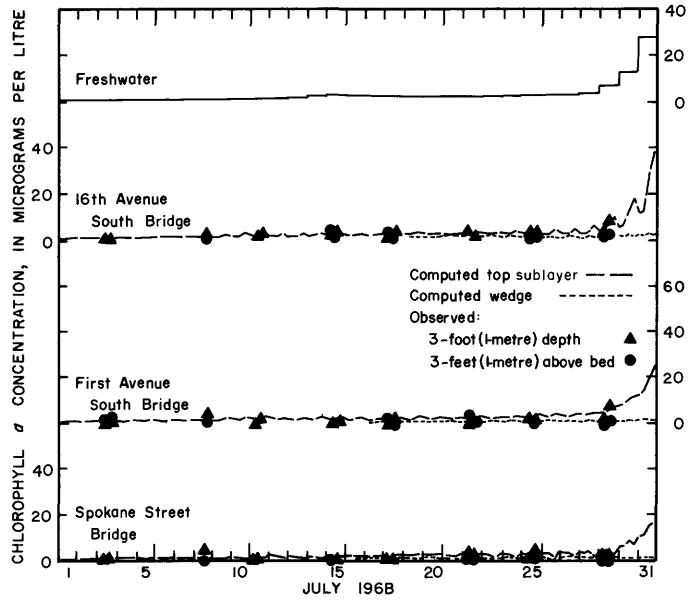

FIGURE 18.—Chlorophyll *a* concentrations in Duwamish River estuary computed at times of high and low tides and observed about twice a day two times per week during July 1968.

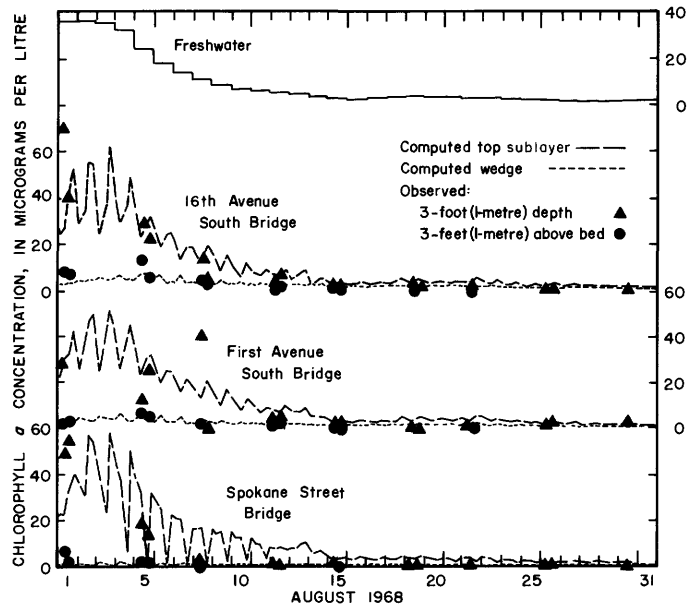

FIGURE 19.—Chlorophyll *a* concentrations in Duwamish River estuary computed at times of high and low tides and observed about twice a day two times per week during August 1968.

South and Spokane Street Bridges follow the trends in the concentrations in the freshwater inflow. Variations within a day, due to the effects of tides or solar-radiation intensity, are apparent in both the computed and observed data.

TEMPERATURE

The computed temperatures as shown in figures 7, 8,

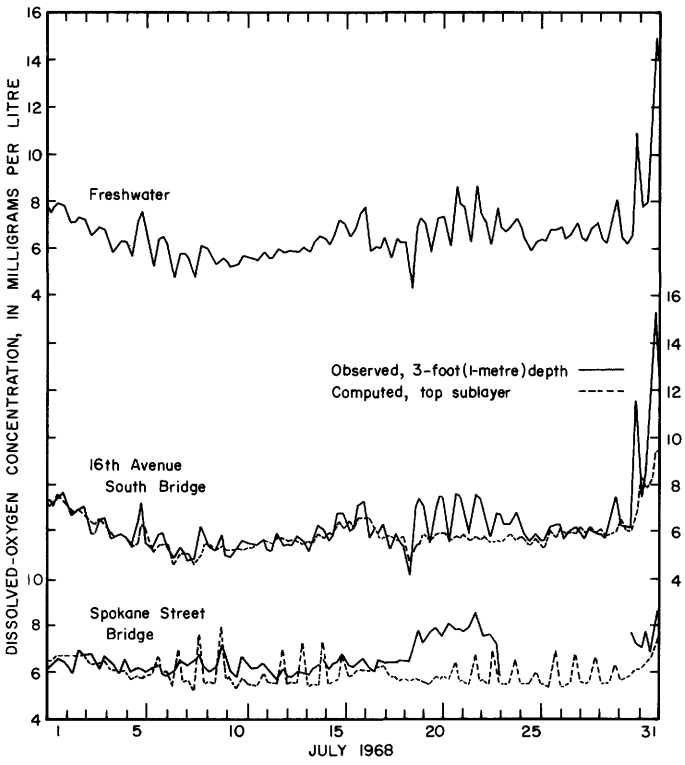

FIGURE 20.—Dissolved oxygen concentrations in Duwamish River estuary at times of high and low tides during July 1968.

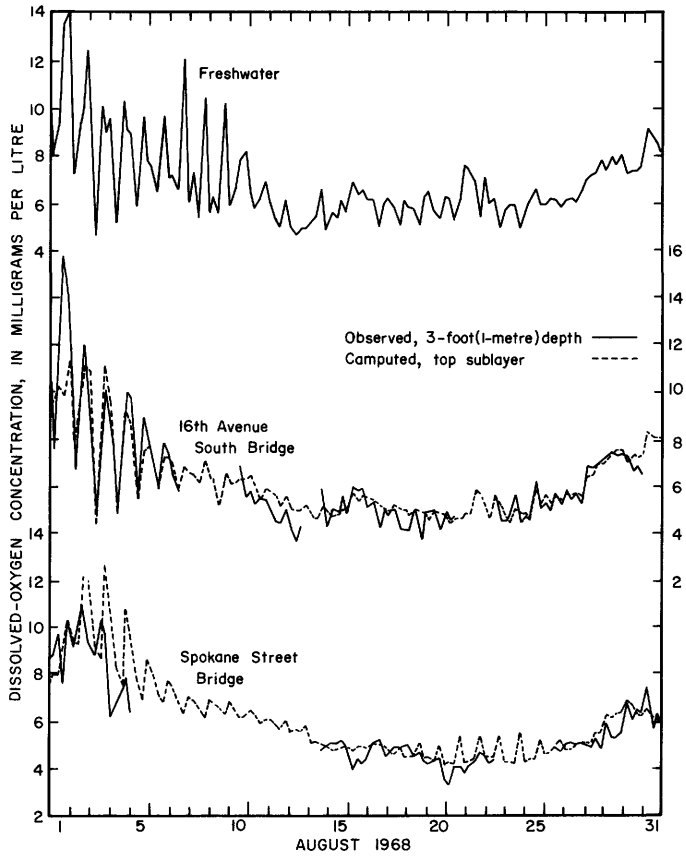

FIGURE 21.—Dissolved-oxygen concentrations in Duwamish River estuary at times of low and high tides during August 1968.

16, 17, and 22 usually agree with the observed temperatures within 2°C, and the daily averages usually agree within about 1°C. High temperatures typically are associated with the less saline water at low tides, and low temperatures with the more saline water at high tides. The association is expected because the seawater in summer is usually cooler than the river water. However, for some unknown reason, high temperatures occasionally are associated with high tide as observed at Spokane Street Bridge in August 1967 (fig. 8); the water there is usually a few degrees cooler than it is at 16th Avenue South Bridge. The temperatures in the wedge, which are not shown in these figures, usually did not vary spacially by more than 1°C. During the summer months, the wedge temperatures were usually between 10° and 14°C.

CHLOROPHYLL *a*

Computed and observed chlorophyll *a* concentrations are compared in figures 9, 10, 11, 18, and 19. Three phytoplankton blooms were observed during these periods, one each in July and August 1967 and one in late July-early August 1968. High DO concentrations, often in excess of the saturation concentrations, are associated with each of the blooms (figs. 12–15, 20–21). During blooms, the chlorophyll *a* concentrations were

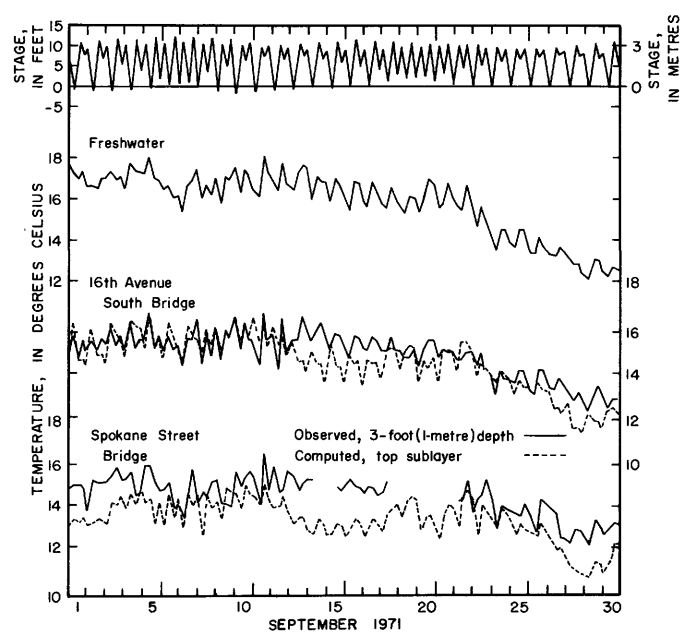

FIGURE 22.—Water temperatures and tide stages in Duwamish River estuary at times of high and low tides during September 1971.

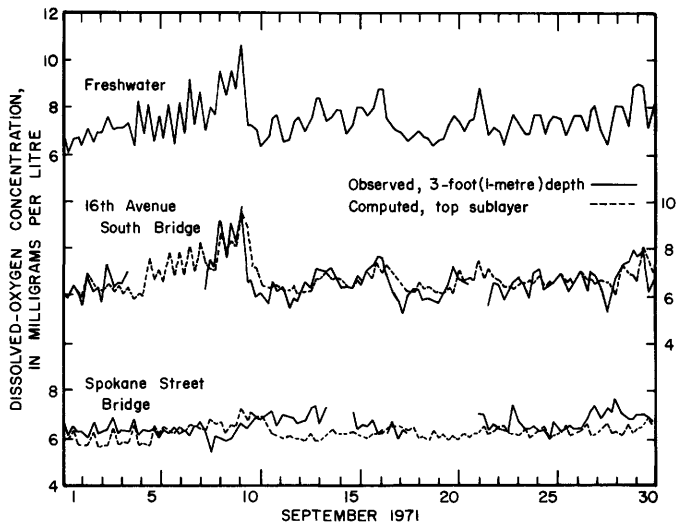

FIGURE 23.—Dissolved oxygen concentrations in Duwamish River estuary at times of high and low tides during September 1971.

much higher in the upper layer than in the wedge. The agreement between the observed and computed chlorophyll *a* concentration data is poorer than that for the temperature data. The larger errors in the phytoplankton model mostly are due to oversimplified mathematical descriptions (equations 26 through 31) of the biological processes and somewhat to the inaccuracies introduced by the insufficient data used to define the boundary conditions for chlorophyll *a*.

The phytoplankton blooms observed at 16th Avenue South, First Avenue South, and Spokane Street Bridges are simulated by the computed data. However, these blooms were not initiated within the modeled region of the estuary; the blooms were inputs to the model in the freshwater inflow and were maintained and advected through the estuary.

Chlorophyll *a* concentration in the upper layer also was modeled without phytoplankton growth in the estuary downstream of the wedge toe. Results of this simulation (not shown in the figures) indicated that chlorophyll *a* and DO concentrations in the upper layer were too low relative to the observed concentrations. Thus, phytoplankton in the estuary downstream of the wedge toe must grow sufficiently to balance the diluting effect of the water entrained from the wedge.

Data for samples taken at East Marginal Way Bridge at low tide when the water there was fresh and at Renton Junction where the water is always fresh rarely show chlorophyll *a* concentrations greater than 10μg/l or supersaturated DO concentrations. However, the chlorophyll *a* concentrations in the freshwater inflow, which are artificial concentrations computed from observed data in the vicinity of the wedge toe, generally were much higher than 10 μg/l during phytoplankton blooms, and the computed DO concentrations in the freshwater inflow often were above saturation levels (figs. 12, 14, 20, 21) during blooms. These differences between the actual freshwater concentrations and the artificial freshwater input concentrations suggest that the brackish-water reach upstream from the wedge toe is an incubator for the phytoplankton that bloom in the estuary. Thus, the biological processes in this brackish-water reach are important in determining the phytoplankton populations in the upper layer of the salt-wedge reach of the estuary.

The agreement between computed and observed chlorophyll *a* concentrations is better for the 1968 bloom than for either of the blooms in 1967. In 1968, the observed bloom at both First Avenue South and at Spokane Street Bridges lasted as long as at 16th Avenue South Bridge, and the magnitudes of the observed chlorophyll *a* concentrations were about the same at the three stations. The input of high chlorophyll *a* concentrations in the freshwater inflow to the estuary during the relatively long 1967 period of blooms generally is confirmed by the observed concentrations at 16th Avenue South Bridge. However, during 1967, observed data show that blooms did not persist as long and chlorophyll *a* concentrations were not as high at First Avenue South and Spokane Street Bridges as at 16th Avenue South Bridge. For example, the August 1967 bloom is barely discernible in the observed data for Spokane Street Bridge (fig. 11). Because the computed chlorophyll *a* concentrations at the two downstream locations closely follow the concentrations at 16th Avenue South Bridge, the computed concentrations at Spokane Street and First Avenue South Bridges are in error for the 1967 blooms.

The reasons for the lack of downstream persistence of the phytoplankton blooms in 1967 as compared to 1968 are not know. Possible explanations include the following: (1) the species that bloomed in the 2 years could have been different, and those that bloomed in 1967 perhaps could not grow well in the more highly saline water of the downstream part of the estuary; (2) herbivores that graze on phytoplankton could have been more numerous in the estuary in 1967 than in 1968; and (3) a toxic substance that inhibits phytoplankton growth could have been present in the lower estuary during 1967 but not in 1968.

The few available data on the phytoplankton species present in the estuary during blooms appear in table 12. Data for the 1968 bloom exist only for the station at First Avenue South Bridge and only for August 5. On that day, the most abundant taxa were oval flagellates that probably were of marine origin. Oval flagellates were also the most abundant taxa at First Avenue

South Bridge during the bloom on August 24, 1967, but not 2 days earlier on August 22, 1967. On this earlier date *Cyclotella* sp., which is of freshwater origin, was most abundant.

The available data on the herbivores in estuary samples on a few days during the blooms of August 1967 and August 1968 (table 13) show similar concentrations of herbivores during both blooms. The phytoplankton loss rate caused by grazing can be estimated by multiplying the filtering rate of an individual organism by the concentration of the grazing organisms. Hutchinson (1967, p. 528) reports filtering rates observed by L. A. Erman for the rotifer *Brachionus calcyciflorus* of 0.002 to 0.014 ml per hour per organism. Thus, the loss rate due to herbivore grazing is approximately

$$(0.005 \text{ ml hr}^{-1} \text{ organisms}^{-1})\ (10 \text{ organisms ml}^{-1}) = 0.05 \text{ hr}^{-1}.$$

Because this value is one-fourth the maximum phytoplankton growth rate used in the model (0.2 hr^{-1}) and is probably nearly as large as the daily average phytoplankton growth rate, grazing by herbivores could be an important mechanism for controlling the phytoplankton populations in the estuary. However, because so few data exist on the concentration of herbivores in the water flowing into the estuary, modeling herbivore populations and their interactions with the phytoplankton in the Duwamish River estuary is not feasible at present.

No data from the Duwamish River estuary are available to support or refute the possibility of toxicants affecting the growth of phytoplankton.

DISSOLVED OXYGEN

Observed and computed DO concentrations are compared in figures 12–15, 20, 21, and 23. The data show daily peaks in the DO concentrations during phytoplankton blooms at both 16th Avenue South and Spokane Street Bridges. During the 1967 period of blooms, the period of computed high DO concentrations lasted a few days longer than the period of high observed concentrations, as did the period of the computed high chlorophyll *a* concentrations. Except during blooms the computed and observed DO concentrations in the upper layer usually agree within about 2 mg/l. The daily means often agree within 1 mg/l.

The wedge DO concentrations (not shown) computed with the present model are nearly identical with those computed previously by Stoner, Haushild, and McConnell (1974) with the earlier version of the model, and the computed and observed concentrations usually agree within 2 mg/l.

PREDICTION OF FUTURE DISSOLVED-OXYGEN CONCENTRATIONS

The model was used to estimate changes in DO concentrations in the estuary in response to an increase in effluent discharge from RTP, with June-September 1971 used as the test period. One set of computations was made using historical input data as described in the preceding section. Another set of computations was made using much of this same data but with some changes to account for the effect of an increased flow from RTP. Four variables changed in the predictions were the flow rate and BOD of the RTP effluent, the DO concentration of the freshwater inflow, and the oxygen consumption rate in the wedge. The changes were estimates based on the designed capacity of RTP and on information provided by Metro personnel, who had given consideration to the available preliminary estimates furnished by their consultants.

For the predictions, the RTP effluent discharge was increased to 223 ft^3/s (6.31 m^3/s) as compared to an average of about 37 ft^3/s (1.05 m^3/s) during June-September 1971. The BOD of the future RTP effluent discharge was assumed to be 5 mg/l as compared to the daily mean of about 3 mg/l (range 1–11 mg/l) during June-September 1971. All freshwater DO concentrations, DO_f, were decreased by 2 mg/l to account for increased oxygen consumption between RTP and the wedge toe and an increased quantity of effluent with a low DO concentration in the freshwater inflow.

Stoner, Haushild, and McConnell (1974) estimate that oxygen in the wedge might be consumed at the rate of 0.27 mg/l per hour for a future RTP effluent discharge of 223 ft^3/s (6.31 m^3/s). For this study their consumption rate was increased to 0.34 mg/l per hour, a 25-percent increase, to account for the increased entrainment rate from the wedge as was described earlier.

Results for both sets of computations for the month of September appear in figure 24. The freshwater DO concentrations shown are all 2 mg/l less than those determined from observed concentrations in September 1971 (fig. 23). The differences between DO concentrations computed with and without increased RTP effluent discharge for Septermber 1971 vary little with time but are less at Spokane Street Bridge than at 16th Avenue South Bridge. Spatial and temporal variations of differences for June-August 1971 (not shown in the figures) were similar to those for September.

The estimated monthly average decreases in DO concentrations in the Duwamish River estuary during June-September 1971 are given in table 8. These decreases are all less than the constant decrease of 2 mg/l assumed for the concentration in the freshwater inflow to the estuary, DO_f. Most of the computed difference is

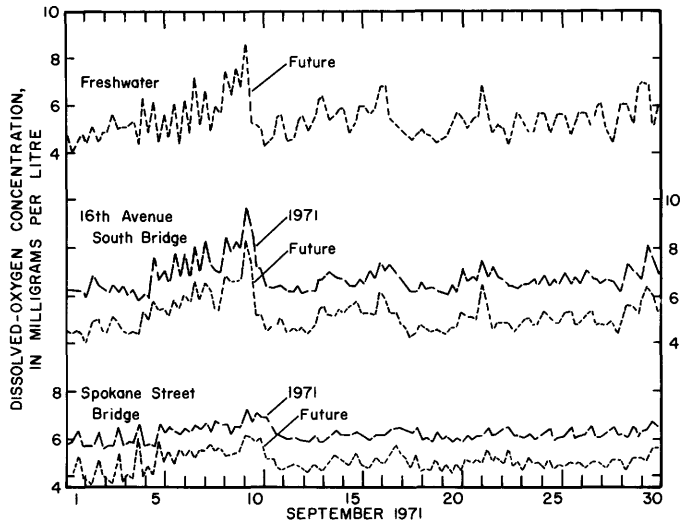

FIGURE 24.—Dissolved-oxygen concentrations in the top sublayer of the Duwamish River estuary model at high and low tides during September 1971, computed for RTP effluent discharges for 1971 (monthly average=35.7 cubic feet per second or 1.01 cubic meters per second) and for the future (223 cubic feet per second or 6.31 cubic meters per second).

caused by the decreased DO of the freshwater inflow and to the increased oxygen consumption in the wedge water which eventually is entrained into the upper layer. The increased consumption of oxygen by the increased BOD in the upper layer accounts for less than 10 percent of the computed difference.

At 16th Avenue South Bridge in the upstream part of the estuary, the decreases in DO concentrations of the top and middle sublayers are influenced mostly by the decrease in DO_f, whereas the decreases in DO concentrations in the bottom sublayer respond more to the decreases in wedge DO concentrations. The average differences at 16th Avenue South Bridge (table 8) were computed using data at times of the high and low tides (usually a total of four times per day). At Spokane Street Bridge near the mouth of the estuary, computed DO concentrations in the wedge and the sublayers at high tide are strongly dependent on the DO concentrations in Elliott Bay. Therefore, the average differences at Spokane Street Bridge (table 8) were computed using only data at times of the low tides.

TABLE 8.—*Estimated decreases in the monthly averages of computed DO concentrations in the Duwamish River estuary during June-September 1971 for an increase in the RTP effluent discharge to the probable future maximum*

Station		Decreases (mg/l) June	July	Aug.	Sept.
16th Avenue South Bridge, averages for high and low tides.	Top sublayer	1.9	1.8	1.7	1.6
	Middle sublayer	1.7	1.7	1.5	1.4
	Bottom sublayer	1.2	1.2	1.3	1.2
	Wedge	.7	.8	1.0	1.1
Spokane Street Bridge, averages for low tides only.	Top sublayer	1.6	1.6	1.5	1.3
	Middle sublayer	1.1	1.3	1.2	1.1
	Bottom sublayer	.5	.7	1.0	.7
	Wedge	.2	.3	.2	.2

Because of a lack of chlorophyll *a* data for 1971, chlorophyll *a* concentrations were not computed for 1971 or for the future when the RTP effluent discharge rate increases. However, because the nutrient concentrations are believed to have been sufficiently high in 1971 so as not to limit the growth of phytoplankton (see section "Supplemental Information"), the increased RTP effluent should not affect the phytoplankton concentrations in the estuary or the amount of oxygen produced or consumed by phytoplankton.

The predictions which were made using estimates of the probable future values of the input data and parameters indicate that the decreases in DO concentrations in the upper layer of the estuary will not be more than the decreases in DO concentration of the freshwater input at the wedge toe. This indication agrees with the relatively unimportant influence of BOD on DO concentrations in the sublayers noted in the modeling of the historical data. Lastly, the predictions were made using preliminary estimates of the effect of future conditions on model inputs and parameters; the confidence in the predictions will increase as these estimates improve.

SUMMARY AND CONCLUSIONS

A numerical model of a salt-wedge estuary developed by Fischer (1974) has been expanded and used to calculate the distributions of salinity, temperature, chlorophyll *a* concentrations, BOD, and DO concentrations in the Duwamish River estuary, King County, Wash. The section of the estuary included in the model extends from the estuary mouth to the toe of the salt-water wedge. The location of the wedge toe, and hence the upstream boundary of the model, is a function of river discharge and tide stage.

In the model, the estuary is divided vertically into the wedge and the upper layer, the latter in turn being divided into three sublayers. Longitudinally, the estuary is divided into about 35 segments; laterally, the estuary is assumed to be homogeneous. The water-transport processes modeled were longitudinal advection and dispersion in the wedge, entrainment from the wedge to the upper layer, longitudinal and vertical advection in the upper layer, and vertical diffusion in the upper layer. These transport processes were computed using conservation of volume equations, observed data, and predicted tide stages.

Additional processes in the model for computing

temperature are heat addition to the water by solar radiation and heat transfer at the surface by long-wave radiation, evaporation, and conduction.

Phytoplankton are modeled as a chlorophyll *a* concentration. The growth of phytoplankton is computed as a function of temperature and light intensity; computed respiration is a function of temperature only. Observed nutrient concentrations are believed to be sufficiently high so that nutrients are not limiting the phytoplankton growth in the estuary. Therefore, nutrients and their effects on phytoplankton were not modeled. The few data on herbivores suggest that their numbers can be sufficiently high to affect the phytoplankton population; however, the data are insufficient to allow the modeling of herbivore populations and their effects on the phytoplankton.

Additional processes in the model for computing DO concentrations in the upper layer are oxygen transfer at the surface, consumption of oxygen by BOD, and the production and consumption of oxygen by phytoplankton during photosynthesis and respiration. In the wedge the model uses a constant oxygen-consumption rate. The BOD in the upper layer of the estuary is low, and its effect on the DO concentration is small. The production of oxygen by photosynthesis in the upper layer is sufficient to cause supersaturation levels of DO during phytoplankton blooms but is relatively unimportant at other times. The effect of phytoplankton respiration on DO concentrations in the Duwamish River estuary is small.

The model was calibrated with data for the summer months of 1968 and verified with data for the summer months of 1967, 1969, and 1971. At any given time the observed and computed temperatures in the upper layer at two stations in the estuary agree within about 2°C, and the daily average temperatures usually agree within 1°C. The computed chlorophyll *a* concentrations increased and decreased with the observed data during a phytoplankton bloom in 1968, but the computed blooms in 1967 persisted farther downstream and lasted a few days longer than did the observed blooms. The blooms are initiated in the brackish waters upstream from the wedge toe and are advected into the modeled reach through the upstream boundary. Thus, the biological processes in the brackish reach upstream from the wedge toe (outside the model boundaries) are important in determining the phytoplankton populations within the modeled reach of the estuary.

Except during bloom periods the computed and observed DO concentrations agreed within about 2 mg/l. During blooms both the computed and observed DO concentrations reached supersaturated levels; however, the error in the computations during the blooms is larger than during periods without blooms.

The effect on the DO concentration of increasing the discharge of treated RTP sewage effluent to the proposed future maximum (223 ft^3/s or 6.3 m^3/s) was estimated with the model. When using the summer data of 1971 as a base, the computed monthly average DO concentrations in the estuary decreased by 2 mg/l or less. Because the concentrations of nutrients in the Duwamish estuary are presently believed to be sufficiently high so as not to limit the growth of phytoplankton, the increase in nutrient concentrations caused by the increased amounts of sewage in the estuary should not affect the phytoplankton growth rates.

REFERENCES

American Public Health Association, American Water Works Association, and Water Pollution Control Federation, 1971, Standard methods for the examination of water and wastewater [13th ed.]: Washington, D.C., 874 p.

Barlow, J. P., Lorenzen, C. J., and Myren, R. T., 1963, Eutrophication of a tidal estuary: Limnology and Oceanography, v. 8, no. 2, p. 251–262.

Bella, D. A., and Grenney, W. J., 1970, Finite difference convection errors: Am. Soc. Civil Engineers Proc., Jour. Sanitary Eng. Div., v. 96, no. SA6, p. 1361–1375.

Chen, C. W., and Orlob, G. T., 1972, Ecologic simulation for aquatic environments, final report: Walnut Creek, California, Water Resources Engineers, Inc., 156 p.

Cupp, E. E., 1943, Marine plankton diatoms of the west coast of North America: Scripps Inst. Oceanography Tech. Ser. Bull. 5 (1), 238 p.

Dawson, W. A., and Tilley, L. J., 1972, Measurement of salt-wedge excursion distance in the Duwamish River estuary, Seattle, Washington, by means of the dissolved-oxygen gradient: U.S. Geol. Survey Water-Supply Paper 1873–D, 27 p.

Di Toro, D. M., O'Connor, D. J., and Thomann, R. V., 1971, A dynamic model of the phytoplankton population in the Sacramento–San Joaquin Delta, *in* Nonequilibrium systems in natural water chemistry: Am. Chem. Soc. Advances in Chemistry Ser. 106, p. 131–180.

Eppley, R. W., Rogers, J.N., and McCarthy, J. J., 1969, Half-saturation constants for uptake of nitrate and ammonium by marine phytoplankton: Limnology and Oceanography, v. 14, no. 6, p. 912–920.

Fair, G. M., Geyer, J. C., and Okun, D. A., 1971, Elements of water supply and wastewater disposal: New York, John Wiley & Sons, Inc., 752 p.

Fischer, H. B., 1972, A Lagrangian method for predicting pollutant dispersion in Bolinas Lagoon, Marin County, California: U.S. Geol. Survey Prof. Paper 582–B, 32 p.

———1975, Description of the model, pt. 1, *in* A numerical model of material transport in salt-wedge estuaries: U.S. Geol. Survey Prof. Paper 917, p. 1–8.

Gibbs, Martin, 1962, Respiration, chap. 4, *in* Lewin, R. A., ed., Physiology and biochemistry of algae: New York, Academic Press, p. 61–90.

Hustedt, Friedrich, 1930, Bacillariophyta (Diatomeae), *in* Süsswasserflora Mitteleuropas: v. 10, chaps. I–VIII, 464 p.

Hutchinson, G. E., 1967, Introduction to lake biology and the limnoplankton, v. II *of* A treatise on limnology: New York, John Wiley & Sons, Inc., 1115 p.

Jitts, H. R., McAllister, C. D., Stephens, K., and Strickland, J. D. H.,

1964, The cell division rates of some marine phytoplankters as a function of light and temperature: Fisheries Research Board Canada Jour., v. 21, no. 1, p. 139–157.

Jobson, H. E., and Sayre, W. W., 1970, Vertical transfer in open channel flow: Am. Soc. Civil Engineers Proc., Jour. Hydraulics Div., v. 96, no. HY3, p. 703–724.

Koberg, G. E., 1964, Methods to compute long-wave radiation from the atmosphere and reflected solar radiation from a water surface: U.S. Geol. Survey Prof. Paper 272–F, p. 107–136.

Kofoid, C. A., and Campbell, A. S., 1929, A conspectus of the marine and fresh-water Ciliata belonging to the sub-order Tintinnoinea, with descriptions of new species principally from the Agassiz Expedition to the eastern tropical Pacific 1904–1905: California Univ. Zoology, pub. 34(1), 404 p.

Lake Tahoe Area Council, 1968, Bioassay of nutrient sources, first progress report *of* Eutrophication of surface waters, Lake Tahoe: South Lake Tahoe, Calif., 178 p.

———1969, Laboratory and pond studies, second progress report *of* Eutrophication of surface waters, Lake Tahoe: South Lake Tahoe, Calif., 180 p.

———1970a, Pilot pond and field studies, third progress report *of* Eutrophication of surface waters, Lake Tahoe: South Lake Tahoe, Calif., 180 p.

———1970b, First progress report *of* Eutrophication of surface waters, Indian Creek Reservoir: South Lake Tahoe, Calif., 141 p.

Leegaard, Cardine, 1915, Untersuchungen über einige Plantoneillinien des Neeres: Nyt. Mag. F. Naturv. L. III 1. 570.5 NV, v. 53–54, 37 p.

MacIsaac, J. J., and Dugdale, R. C., 1969, The kinetics of nitrate and ammonia uptake by natural populations of marine phytoplankton: Deep-Sea Research, v. 16, p. 415–422.

McKee, J. E., and Wolf, H. W., 1963, Water quality criteria: California State Water Quality Control Board Pub. 3–A, 548 p.

Megard, R. O., 1973, Rates of photosynthesis and phytoplankton growth in Shagawa Lake, Minnesota, pub. EPA–R3–73–039 *of* Ecological Research Series of U.S. Environmental Protection Agency: Washington, D.C., U.S. Govt. Printing Office, 70 p.

Nelson, J. E., 1972, Vertical turbulent mixing in stratified flow—a comparison of previous experiments: California Univ. (Berkeley) Dept. Civil Engineering, Hydraulic Eng. Lab., Waste Heat Management Rept. Ser., Rept. No. WHM–3, 33 p.

Platt, Trevor, 1969, The concept of energy efficiency in primary production: Limnology and Oceanography, v. 14, no. 5, p. 653–659.

Richards, F. A., and Thompson, T. G., 1952, A spectrophotometric method for the estimation of plankton pigments; pt. 2, The estimation and characterization of plankton population by pigment analysis: Jour. Marine Research, v. 11, no. 2, p. 156–172.

Ryther, J. H., 1956, Photosynthesis in the ocean as a function of light intensity: Limnology and Oceanography, v. 1, no. 1, p. 61–70.

———1963, Geographic variations in productivity, *in* Ideas and observations on progress in the study of the seas, Volume 2 of Hill, M. N., ed., The Sea: New York, Interscience Publishers, p. 347–380.

Ryther, J. H., and Yentsch, C. S., 1957, The estimation of phytoplankton production in the ocean from chlorophyll and light data: Limnology and Oceanography, v. 2, no. 3, p. 281–286.

Santos, J. F., and Stoner, J. D., 1972, Physical, chemical, and biological aspects of the Duwamish River estuary, King County, Washington, 1963–67: U.S. Geol. Survey Water-Supply Paper 1873–C, 74 p.

Schiller, Josef, 1930, Coccolithineae, *in* Rabenhorst's Kryptogamen-Flora von Deutschland, Österreich und der Schweiz, 10(2): p. 89–267.

Shimada, B. M., 1958, Diurnal fluctuation in photosynthetic rate and chlorophyll *a* content of phytoplankton from eastern Pacific waters: Limnology and Oceanography, v. 3, no. 3, p. 336–339.

Slack, K. V., Averett, R. C., Greeson, P. E., and Lipscomb, R. G., 1973, Methods for collection and analysis of aquatic biological and microbiological samples: U.S. Geol. Survey Water-Resources Inv. Techniques, book 5, chap. A–4, 165 p.

Steele, J. H., 1962, Environmental control of photosynthesis in the sea: Limnology and Oceanography, v. 7., no. 2, p. 137–150.

Stoner, J. D., 1972, Determination of mass balance and entrainment in the stratified Duwamish River estuary, King County, Washington: U.S. Geol. Survey Water-Supply Paper 1873–F, 17 p.

Stoner, J. D., Haushild, W. L., and McConnell, J. B., 1975, Model computation of salinity and salt-wedge dissolved oxygen in the lower Duwamish River estuary, King County, Washington, pt. II, *in* A numerical model of material transport in salt-wedge estuaries: U.S. Geol. Survey Prof. Paper 917, p. 11–36.

Strickland, J. D. H., 1960, Measuring the production of marine phytoplankton: Fisheries Research Board Canada Bull. 122, p. 5–22 and 95–100.

Strickland, J. D. H., and Parsons, T. R., 1968, A practical handbook of seawater analysis: Fisheries Research Board Canada Bull. 167, 311 p.

Sverdrup, H. V., Johnson, M. W., and Fleming, R. H., 1961, The oceans, their physics, chemistry, and general biology: Englewood Cliffs, New Jersey, Prentice-Hall, Inc., 1087 p.

Talling, J. F., 1962, Freshwater algae, *in* Lewin, R. A., ed., Physiology and biochemistry of algae: New York, Academic Press, p. 743–757.

Thames Survey Committee and Water Pollution Research Laboratory, 1964, Effects of polluting discharges on the Thames estuary: Water Pollution Research Technical Paper No. 11, London, Her Majesty's Stationery Office, 609 p., 1 pl.

Tilley, L. J., and Dawson, W. A., 1971, Plant nutrients and the estuary mechanism in the Duwamish River estuary, Seattle, Washington, *in* Geological Survey research, 1971: U.S. Geol. Survey Prof. Paper 750–C, p. C185–C191.

[U.S.] Environmental Science Services Administration, 1967–69, Tide tables, high and low water predictions, west coast of North and South America including the Hawaiian Islands: Washington, D.C., U.S. Govt. Printing Off., pub. annually.

———1967–69, Local climatological data: Washington, D.C., U.S. Govt. Printing Office, pub. monthly.

[U.S.] National Oceanic and Atmospheric Administration, 1971, Local climatological data: Washington, D.C., U.S. Govt. Printing Office, pub. monthly.

Verduin, Jacob, 1956, Primary production in lakes: Limnology and Oceanography, v. 1, no. 2, p. 85–91.

Wailes, G. H., 1939, Canadian Pacific fauna, 1. Protozoa: 1a, lobosa, 1b, regiculoza, 1c, heliozoa, 1d, radiolaria, 1e, mastigophora, 1f, ciliata, lg, suctoria: Fisheries Research Board Canada, Toronto, Univ. Toronto Press, 104 p.

Ward, H. B., and Whipple, G. C., 1959, Fresh water biology, edited by W. T. Edmondson 2d ed.: New York, John Wiley & Sons, Inc., 1248 p.

Welch, E. B., 1969, Factors initiating phytoplankton blooms and resulting effects on dissolved oxygen in Duwamish River estuary, Seattle, Washington: U.S. Geol. Survey Water-Supply Paper 1873–A, 62 p.

Yotsukura, Nobuhiro, Jackman, A. P., and Faust, C. R., 1973, Approximation of heat exchange at the air-water interface: Water Resources Research, v. 9, no. 1, p. 118–128.

SUPPLEMENTAL INFORMATION

PHYTOPLANKTON

GENERAL

Slack, Averett, Greeson, and Lipscomb (1973) define phytoplankton as the community of suspended or floating plant organisms that drift passively with water currents. The Duwamish River estuary contains phytoplankton species of both freshwater and marine origin; the former enter the estuary with the water from the Green-Duwamish River, and the latter enter from Elliott Bay. Only suspended phytoplankton are discussed in this report; phytoplankton that float on the surface are not of importance in the Duwamish River estuary at present.

During their stay in the estuary, phytoplankters may grow, produce oxygen by photosynthesis, decrease in mass and consume oxygen by respiration, be transported by currents, settle, and be eaten by grazers. The eventual fate of the phytoplankton not eaten by grazers in the estuary is either being transported into Elliott Bay or becoming a part of the streambed sediment.

Phytoplankton growth and photosynthesis occur mainly in the upper layer of the estuary. Although the top part of the saltwater wedge is within the photic zone, light in most of the wedge is insufficient to support active phytoplankton photosynthesis (Welch, 1969). The growth of phytoplankton and the production of oxygen by photosynthesis are the important biological processes in the model. Although modeled, the use of oxygen and the decrease in biomass attributed to respiration are less important biological processes in the estuary. Grazing was not modeled. Phytoplankton photosynthesis increases DO concentrations in the estuary significantly during blooms but has a negligible effect on DO concentration during nonbloom periods. A phytoplankton bloom, as defined in this report, is either 0.5 million or more cells per litre (as defined by Slack and others, 1973) or a chlorophyll *a* concentration in excess of 4 μg/l (as defined by Welch, 1969) during a continuous period longer than a day.

SAMPLE COLLECTION, PREPARATION, AND ANALYSIS

The concentrations of chlorophyll *a* and other pigments were determined for water samples collected in the Green-Duwamish River and in Elliott Bay. The plant-pigment data were supplemented by phytoplankton cell counts and taxonomic identification for selected samples.

The river samples were collected during 1967–69, usually at six stations starting at Spokane Street Bridge and ending at the Renton Junction monitor (fig. 1). The Elliott Bay samples were collected by Metro personnel (under the direction of R. I. Matsuda) at four stations during the April-June periods of 1967–69. Bay samples were collected from depths of about 3 ft (1 m) and river samples were collected from about 3 ft (1 m) below the water surface (surface samples), or about 3 ft (1 m) above the streambed (bottom samples). Samples at most stations were collected with the Emsworth version of a 4-litre Van Dorn sampler. However, many river samples were obtained from the pumped stream supplying the automatic water-quality monitors.

Immediately after sample collection, a 125 ml aliquot was preserved with Lugol's solution for cell counting and identification. Phytoplankton were identified and counted by W. A. Dawson and L. J. Tilley using the inverted-microscope technique (Slack and others, 1973).

For analysis of plant pigments, volumes between 0.5 and 4.0 litres were filtered through 0.45-μm membrane filters. The river samples were filtered at about one-half atmosphere of positive pressure within 1 hour of the time of collection. The bay samples were subjected to slightly greater delay before filtration in a vacuum apparatus at no more than one-fifth atmosphere negative pressure. The folded filters containing the phytoplankton were stored in desiccators at 5°C. Acetone extracts from the filter and samples were analyzed for plant pigments by the method of Richards with Thompson (1952), as modified by Strickland and Parsons (1968).

The work of Ward and Whipple (1959) was the most useful reference for identification of freshwater organisms. Marine organisms were identified with the aid of the works of Cupp (1943), Wailes (1939), Hustedt (1930), Schiller (1930), Leegaard (1915), and Kofoid and Campbell (1929).

ABUNDANT PHYTOPLANKTON TAXA

The most abundant organisms found in Elliott Bay samples (table 9) were *Skeletonema costatum* and *Thalassiosira* sp. The samples listed in table 9 were selected for taxonomic analysis to represent times of peak chlorophyll *a* concentrations in the surface waters of Elliott Bay near Seattle during the April-June periods of 1967–69 (R. I. Matsuda, Metro, oral commun., 1971). Although the data in table 9 are for spring months, the two dominant genera probably enter the Duwamish River estuary with the bay water not only in the spring but in summer and early fall as well. Welch (1969) identified *Skeletonema* as the most abundant taxa in samples from 16th Avenue South Bridge during a bloom in early August 1965 and speculated that an abundant diatom might be *Thalassiosira* in a later bloom during the same month. *Skeletonema* was one of the abundant organisms in samples from some estuary stations during blooms in August 1967 (table 12).

The list of abundant freshwater organisms in samples from the Green-Duwamish River during March-August 1967 (table 10) shows a diversity of dominant genera. Several genera appear in both listings of abundant taxa in samples from the two stations in the freshwater part of the river (tables 10, 11). Many organisms found in the freshwater samples from the river must have been periphyton which had been dislodged upstream and subsequently carried downstream by the river currents.

The abundant organisms in samples from six stations on the estuary and river during 2 days of an August 1967 bloom and from one estuary station during 1 day of an August 1968 bloom are listed in table 12. The diversity in the abundant river taxa is again evident by the data for samples from the Renton Junction monitor station and East Marginal Way Bridge. The marine diatom, *Skeletonema costatum,* was one of the abundant species only in the samples collected from the two farthest downstream stations on August 22, 1967.

Cyclotella sp. and oval flagellates, along with "coccoids," dominate the abundance listing for the estuary during the August 1967 blooms. *Cyclotella* sp., a freshwater diatom, was not numerous enough to be listed among the abundant freshwater organisms (tables 10, 11); it ranked about ninth in abundance of the freshwater autotrophic organisms found in the Green-Duwamish River. The oval flagellates were probably marine organisms from Elliott Bay; oval flagellates were the 20th most abundant autotrophic organism found in the bay samples of the April-June periods of 1967–69. However, because the taxonomic analyses of the estuary samples may not have distinguished between freshwater and marine oval flagellates, the probable origin of these microorganisms is designated in table 12 as "saltwater(?)" to indicate some uncertainty. Regardless of their origin, both *Cyclotella* sp. and oval flagellates flourished in brackish estuary water having a wide range in salinity.

The longitudinal distributions of *Cyclotella* sp. (fig. 25) indicate a peak concentration in the brackish surface water between Boeing Bridge (mile 6.5 or kilometre 10.5) and First Avenue South Bridge (mile 3.4 or kilometre 5.5). Downstream of this reach, the consistently lower concentrations at Spokane Street Bridge indicate that the prevailing high salinity there may limit the growth of this diatom. Upstream of the peak-concentration reach, the concentration

TABLE 9.—*Abundant taxa in samples collected at four stations in Elliott Bay near Seattle during 1967–69*

[Phytoplankton samples collected by R. I. Matsuda, Municipality of Metropolitan Seattle, and counted and identified by W. A. Dawson and L. J. Tilley]

Date	Chlorophyll *a* concentration (μg/l)	Taxon	Concentration		Presence of bloom
			Cells/ml	Percentage of total	
1967					
May 17	5.3	*Skeletonema costatum*	480	47	No
		Thalassiosira sp	400	39	No
May 17	4.1	*Skeletonema costatum*	1,500	74	Yes
		Thalassiosira sp	430	22	No
1968					
Apr. 29	*9.8*	*Skeletonema costatum*	610	41	Yes
		Thalassiosira sp	460	31	No
Apr. 29	3.3	*Skeletonema costatum*	850	75	Yes
		Flagellate, oval	170	15	No
May 27	11.4	*Skeletonema costatum*	7,700	88	Yes
		Thalassiosira sp	610	7	Yes
May 27	9.2	*Skeletonema costatum*	2,400	68	Yes
		Thalassiosira sp	840	24	Yes
June 3	11.7	do	1,600	66	Yes
		Skeletonema costatum	360	15	No
1969					
May 14	4.6	do	12,000	98	Yes
May 14	3.6	do	12,000	98	Yes
May 21	2.3	do	4,700	91	Yes
		Chaetoceros sp	370	7	No
May 21	3.5	*Skeletonema costatum*	4,700	86	Yes
		Chaetoceros sp	660	12	Yes

TABLE 10.—*Abundant taxa in 1967 freshwater samples from two stations on the Green-Duwamish River*

[Taxa counted and identified by W. A. Dawson and L. J. Tilley]

Date	Time (P.s.t.)	Chlorophyll *a* concentration (μg/l)	Taxon	Concentration		Presence of bloom
				Cells/ml	Percentage of totals	
Renton Junction Monitor (mi 13.1, km 21.1						
Mar. 14	1020	0.8	Unidentified blue-green algae.	2,500	50	Yes
Apr. 18	1035	3.8	*Hannaea* sp	34	27	No
May 12	1200	2.5	Pennate diatoms	90	17	No
24	1425	3.6	Unidentified blue-green algae	7,800	71	Yes
June 8	1245	1.8	*Chrysococcus* sp	350	23	No
27	0805	3.6	"Coccoids" and clusters	2,300	40	Yes
July 5	0820	4.0	*Oscillatoria* sp	1,700	34	Yes
11	0800	3.7	"Coccoids" and clusters	1,500	29	Yes
25	1245	4.5	Flagellate spp	2,200	31	Yes
Aug. 22	1630	2.7	"Coccoids," solitary	5,600	61	Yes
East Marginal Way Bridge[1] (mi 7.8, km 12.6)						
Mar. 14	1040	0.5	*Crenothrix* sp	700	87	Yes
May 12	1245	2.5	*Synedra* sp	54	13	No
24	1020	2.2	*Oscillatoria* sp	190	36	No
June 20	0830	2.2	do	930	38	Yes
July 5	0845	3.3	"Coccoids" and clusters	840	25	Yes
25	1225	6.0	Flagellate sp	3,900	36	Yes

[1]Samples obtained during low tides when river did not contain saltwater here.

of *Cyclotella* sp. is lower at East Marginal Way Bridge, mile 7.8 or km 12.6 (concentration being tide-dependent here), and decreases rapidly thereafter with distance upstream.

Longitudinal distributions of oval flagellates (fig. 26) indicate peak concentrations downstream from Boeing Bridge (mile 6.5 or kilometre 10.5) with the concentration at Spokane Street Bridge (mile 1.2 or kilometre 1.9) either higher or only slightly less than concentrations at adjacent upstream stations. The rapid decrease in concentration of oval flagellates with distance upstream from Boeing Bridge suggests that they are marine organisms reacting to the increasingly fresher water. In general, the concentration of "coccoids" decreases downstream and, therefore, with increasing salinity (fig. 27).

TABLE 11.—*Five most abundant taxa in freshwater samples obtained at two stations on the Green-Duwamish River during March-August 1967*

[Taxa counted, identified, and ranked by W. A. Dawson and L. J. Tilley]

Abundance ranking	Taxon and sampling station	
	Renton Junction Monitor (mi 13.1, km 21.1)	East Marginal Way Bridge (mi 7.8, km 12.6)
1	"Coccoids" and clusters	*Oscillatoria* sp.
2	*Micractinium* sp	Pennate diatoms.
3	*Scenedesmus* spp	*Scenedesmus* spp.
4	*Golenkinia* sp	"Coccoids" and clusters.
5	*Oscillatoria* sp	*Chlamydomonas* sp.

PRODUCTION AND CONSUMPTION OF OXYGEN BY PHYTOPLANKTON

When blooming, the phytoplankton in the upper layer of the Duwamish River estuary produce more oxygen by photosynthesis than they consume by respiration, frequently resulting in DO supersaturation. DO supersaturation has not been observed in the wedge.

In the model the production of oxygen during photosynthesis is assumed to be proportional to the increase in chlorophyll *a* concentration caused by phytoplankton growth. Similarly, the consumption of oxygen during respiration is assumed to be proportional to the decrease in chlorophyll *a* concentration. The coefficient of proportionality was assumed to be the same for both processes, which implies a photosynthesis-to-respiration ratio of unity for stable populations. The coefficient of proportionality relating the increase of DO to chlorophyll *a*, which is denoted by DO_C in the main body of this report, was estimated from data obtained in the Duwamish River and estuary during phytoplankton blooms. The procedure used is as follows:

1. The salinity, DO concentration, and the chlorophyll *a* concentration, S_b, DO_b, and CP_b, were observed at a point in the river or estuary where there was a bloom. The salinity and DO concentration were observed at two other points, one upstream from the first where there was no bloom, S_u and DO_u, and the other in the wedge, S_w and DO_w. The chlorophyll *a* concentrations at the second two points usually were not observed but were known to be a small fraction of the concentration at the first point.
2. The relative volumes of water from the upstream point, V_u, and from the wedge point, V_w, required to produce a mixture of salinity, S_b, was computed as

$$V_u = \frac{S_w - S_b}{S_w - S_u} \quad \text{and} \quad V_w = 1 - V_u .$$

3. The DO concentration of this mixture, DO_m, was computed as

$$DO_m = V_u\, DO_u + V_w\, DO_w .$$

4. The excess DO concentration, defined as $\Delta DO = DO_b - DO_m$, was plotted as a function of the chlorophyll *a* concentration CP_b (fig. 28).
5. If one assumes that the excess DO concentration is the net increase in oxygen concentration due only to phytosynthesis and respiration of the phytoplankton during the production of all the chlorophyll *a* at the bloom point, then, the slope of the line fit to the data in figure 28 is an average measure of the desired coefficient of proportionality, DO_C. The available data from the

TABLE 12.—*Abundant taxa during two blooms in the Green-Duwamish River*

[Phytoplankton counted and identified by W. A. Dawson]

Date	Station	Time (P.s.t.) and tide stage	Depth location[1]	Salinity (ppt)	Chlorophyll *a* concentration (μg/l)	Taxon	Concentration: Cells/ml	Concentration: Percentage of total[2]	Probable origin	Presence of bloom
1967										
Aug. 22	Renton Junction Monitor.	1530 Midflood	Surface	0	2.6	*Micractinium* sp	710	42	Freshwater	Yes
						Oscillatoria sp.	510	30	do	Yes
						("Coccoids" and clusters)	(6,700)	(398)	do	Yes
	East Marginal Way Bridge.	0930 Late ebb	do	.2	10.5	*Cyclotella* sp	5,300	88	do	Yes
						Chlamydomonas sp	410	7	do	No
						("Coccoids" and clusters)	(2,800)	(47)	do	Yes
		1520 Midflood	do	.4	11.3	*Melosira* sp	1,600	56	do	Yes
						Chrysococcus sp	980	35	do	Yes
	Boeing Bridge.	0915 Late ebb	do		41.3	*Cyclotella* sp	31,000	98	do	Yes
						("Coccoids" and clusters)	(1,400)	(4)	do	Yes
		1425 Midflood	do	.8	21.9	*Cyclotella* sp	33,000	93	do	Yes
						Chlamydomonas sp	1,200	3	do	Yes
						("Coccoids" and clusters)	(3,900)	(11)	do	Yes
	16th Avenue South Bridge.	0845 Midebb	do	16.7	5.6	*Cyclotella* sp	13,000	98	do	Yes
						("Coccoids" and clusters)	(3,700)	(3)	do	Yes
		1400 Early flood	do	12.9	37.8	*Cyclotella* sp	57,000	98	do	Yes
						Flagellate, oval 5–7 μm	510	1	Saltwater(?)	Yes
						("Coccoids" and clusters)	(1,800)	(3)	Freshwater	Yes
		1405 Early flood	Bottom	26.4	3.5	*Cyclotella* sp	690	71	do	Yes
						Navicula spp	110	11	do	No
						("Coccoids" and clusters)	(1,200)	(123)	do	Yes
	First Avenue South Bridge.	0825 Midebb	Surface	20.5	6.6	*Cyclotella* sp	13,000	92	do	Yes
						Skeletonema costatum	1,000	7	Saltwater	Yes
						("Coccoids" and clusters)	(2,400)	(18)	Freshwater	Yes
		1340 Early flood	do	13.0	15.6	*Cyclotella* sp	39,000	99	do	Yes
						("Coccoids" and clusters)	(2,000)	(5)	do	Yes
		1345 Early flood	Bottom	27.4	1.2	*Cyclotella* sp	550	77	do	Yes
						("Coccoids" and clusters)	(55)	(8)	do	No
	Spokane Street Bridge.	0735 Early ebb	Surface	24.0	2.0	*Skeletonema costatum*	1,400	54	Saltwater	Yes
						Cyclotella sp	1,200	46	Freshwater	Yes
		1305 Early ebb	do	23.3	5.5	*Cyclotella* sp	2,000	50	do	Yes
						Skeletonema costatum	1,100	26	Saltwater	Yes
						Flagellate, oval 5–7 μm	550	14	Saltwater(?)	Yes
						("Coccoids" and clusters)	(310)	(8)	Freshwater	No
		0755 Early ebb	Bottom	28.5	1.8	Flagellate, oval 6–8 μm	200	39	Saltwater(?)	No
						Chilomonas sp	97	19	Saltwater	No
						Skeletonema costatum	89	18	do	No
		1310 Early flood	do	28.4	.9	Flagellate, oval 6–8 μm	61	51	Saltwater(?)	No
						Chilomonas sp	23	19	Saltwater	No
Aug. 24	Renton Junction Monitor.	0930 Early ebb	Surface	0	6.7	*Scenedesmus*	1,100	91	Freshwater	Yes
						("Coccoids" and clusters)	(990)	(85)	do	Yes
		1540 Early flood	do	0	9.6	*Scenedesmus*	3,400	90	do	Yes
						("Coccoids and clusters)	(12,000)	(321)	do	Yes
	East Marginal Way Bridge.	0190 Early ebb	do	1.7	21.9	Flagellate, oval 5–7 μm	11,000	53	Saltwater(?)	Yes
						Cyclotella sp	8,900	44	Freshwater	Yes
						("Coccoids" and clusters)	(5,800)	(28)	do	Yes
		1525 Early ebb	do	.2	8.4	*Scenedesmus*	2,600	46	do	Yes
						Cyclotella sp	2,100	38	do	Yes
						Chlamydomonas	470	8	do	No
						("Coccoids" and clusters)	(4,000)	(72)	do	Yes
	Boeing Bridge.	0830 Start of ebb	do	11.0	47.8	Flagellate, oval 5–7 μm	80,000	97	Saltwater(?)	Yes
						Cyclotella sp	2,200	3	Freshwater	Yes
						("Coccoids" and clusters)	(5,400)	(7)	do	Yes
		1440 Start of flood	do	.8	13.2	*Cyclotella* sp	4,600	61	do	Yes
						Scenedesmus	2,400	32	do	Yes
						Flagellate, oval 5–7 μm	710	10	Saltwater(?)	Yes
						("Coccoids" and clusters)	(3,300)	(45)	Freshwater	Yes
	16th Avenue South Bridge.	0805 Low high	dc	14.7	33.7	Flagellate, oval 5–7 μm	77,000	99	Saltwater(?)	Yes
						Cyclotella sp	150	<1	Freshwater	No
						Scenedesmus	110	<1	do	No
						("Coccoids" and clusters)	(42)	(<1)	do	No
		0815 Low high	Bottom	27.7	3.9	Flagellate, oval 5–7 μm	1,700	87	Saltwater(?)	Yes
						("Coccoids" and clusters)	(190)	(1)	Freshwater	No
		1415 Low low	Surface	7.4	58.9	*Cyclotella* sp	66,000	94	do	Yes
						Flagellate, oval 5–7 μm	3,000	4	Saltwater(?)	Yes
						("Coccoids" and clusters)	(360)	(1)	Freshwater	No
		1425 Low low	Bottom	26.7	5.6	Flagellate, oval 3–5 μm	1,100	61	Saltwater(?)	Yes
						Cyclotella sp	250	14	Freshwater	No
						("Coccoids" and clusters)	(91)	(5)	do	No
	First Avenue South Bridge.	0740 Low high	Surface	16.7	10.0	Flagellate, oval 5–7 μm	12,000	99	Saltwater(?)	Yes
						("Coccoids" and clusters)	(140)	(<1)	Freshwater	No
		0750 Low high	Bottom	28.0	2.6	Flagellate, oval 5–7 μm	840	82	Saltwater(?)	Yes
						("Coccoids" and clusters)	(25)	(2)	Freshwater	No
		1345 Low low	Surface	11.5	66.8	*Cyclotella* sp	110,000	99	do	Yes
						Flagellate, oval 5–7μm	1,000	<1	Saltwater(?)	Yes
						("Coccoids" and clusters)	(510)	(<1)	Freshwater	Yes
		1355 Low low	Bottom	28.1	1.6	Flagellate, oval 5–7 μm	37	83	Saltwater(?)	No
						("Coccoids" and clusters)	(15)	(34)	Freshwater	No

TABLE 12.—*Abundant taxa during two blooms in the Green-Duwamish River*—Continued

Date	Station	Time (P.s.t.) and tide stage	Depth location[1]	Salinity (ppt)	Chlorophyll *a* concentration (μg/l)	Taxon	Concentration: Cells/ml	Concentration: Percentage of total[2]	Probable origin	Presence of bloom
	Spokane Street Bridge.	0645 Low high	Surface	21.8	9.5	Flagellate, oval 5–7 μm	25,000	97	Saltwater(?)	Yes
						Cyclotella sp	300	1	Freshwater	No
		0705 Low high	Bottom	28.7	.3	Flagellate, oval 5–7 μm	36	40	Saltwater(?)	No
						Chilomonas sp	23	26	Saltwater	No
						("Coccoids" and clusters)	(6)	(7)	Freshwater	No
		1310 Low low	Surface	23.4	9.0	Flagellate, oval 5–7 μm	18,000	90	Saltwater(?)	Yes
						Cyclotella sp	1,800	9	Freshwater	Yes
						("Coccoids" and clusters)	(15,000)	(74)	do	Yes
		1320 Low low	Bottom	28.3	.9	Flagellate, oval 6–8 μm	88	41	Saltwater(?)	No
						Peridinium	83	38	Saltwater	No
						Chilomonas sp	31	14	do	No
1968										
Aug 5	First Avenue South Bridge.	0940 Low low	Surface	12.9	13.2	Flagellate, oval 6–10 μm	19,000	95	Saltwater(?)	Yes
						Cyclotella sp	720	4	Freshwater	Yes
		1830 Early ebb	do	27.3	26.0	Flagellate, oval 6–10 μm	16,000	96	Saltwater(?)	Yes
						Cyclotella sp	480	3	Freshwater	No

[1]Surface and bottom indicate about 3 feet (1 m) below water surface and about 3 feet (1 m) above streambed, respectively.
[2]Total is sum of concentrations for the various taxa counted but does not include concentration of "coccoids" and "coccoid" clusters.

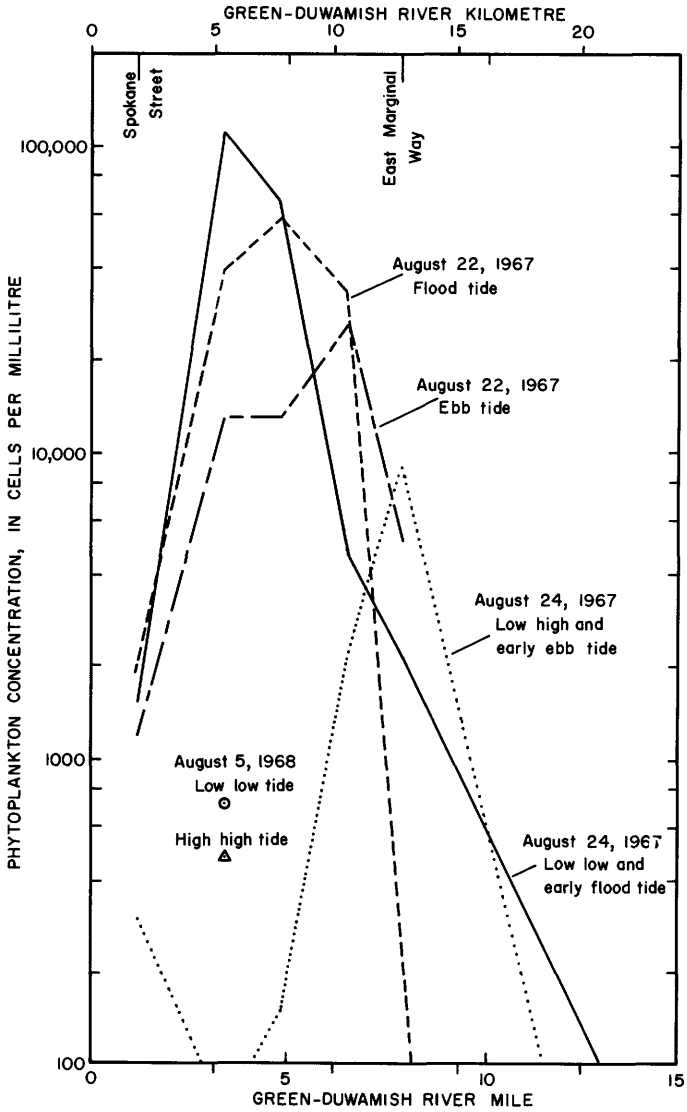

FIGURE 25.—Longitudinal distributions of *Cyclotella* sp. during a bloom in 1967 and data at two points during a bloom in 1968.

Duwamish River estuary yield DO_C=0.125 mg oxygen per microgram chlorophyll *a*.

ESTIMATED INFLUENCE OF NUTRIENTS ON PHYTOPLANKTON GROWTH

The effluent from RTP considerably increases concentrations of ammonium and total and soluble phosphate in the Duwamish River estuary (Welch, 1969, fig. 8; Tilley and Dawson, 1971, fig. 3) but does not greatly increase the concentration of nitrate (Welch, 1969, fig. 8; Santos and Stoner, 1972, p. 62–63). The nutrients contributed by the RTP effluent have the potential of increasing the phytoplankton biomass in the estuary. Welch (1969) reported that the addition of RTP effluent to Duwamish River estuary samples increased the population of a green-algae population (*Scenedesmus* sp.) when the samples were incubated in flasks under uniform light of about 7,000 lux and a temperature of 20°–21°C, without mixing for 5 or 6 days. In one series of tests, the maximum assimilated carbon-14 (a measure of the biomass produced) in samples containing 5-, 10- and 25-percent RTP effluent was about 14, 30, and 36 percent greater than in samples without effluent. Welch (1969) also stated that the observed data for chlorophyll *a* concentration in the estuary showed no significant increase in the estuary's phytoplankton biomass following a 46-percent increase in effluent discharge between 1965 and 1966. Later data suggest that chlorophyll *a* concentrations (figs. 9–11, 18, 19) and cell concentrations (table 12) in the 1967–68 blooms were at about the same level as they were in the 1965–66 blooms (Welch, 1969, figs. 3, 5). As Welch also noted, it is impossible to make definitive comparisons between maximum biomass of blooms because of the difficulty of sampling the maximum biomass for any one bloom.

Computed Michaelis-Menton factors were used in estimating the effects of nutrients on growth rates of phytoplankton in the Duwamish River estuary. These and similar factors, like F_L or F_T, can be included in equation 29 for reducing the growth rate because of deficiency of a nutrient or the effects of any other parameter. The

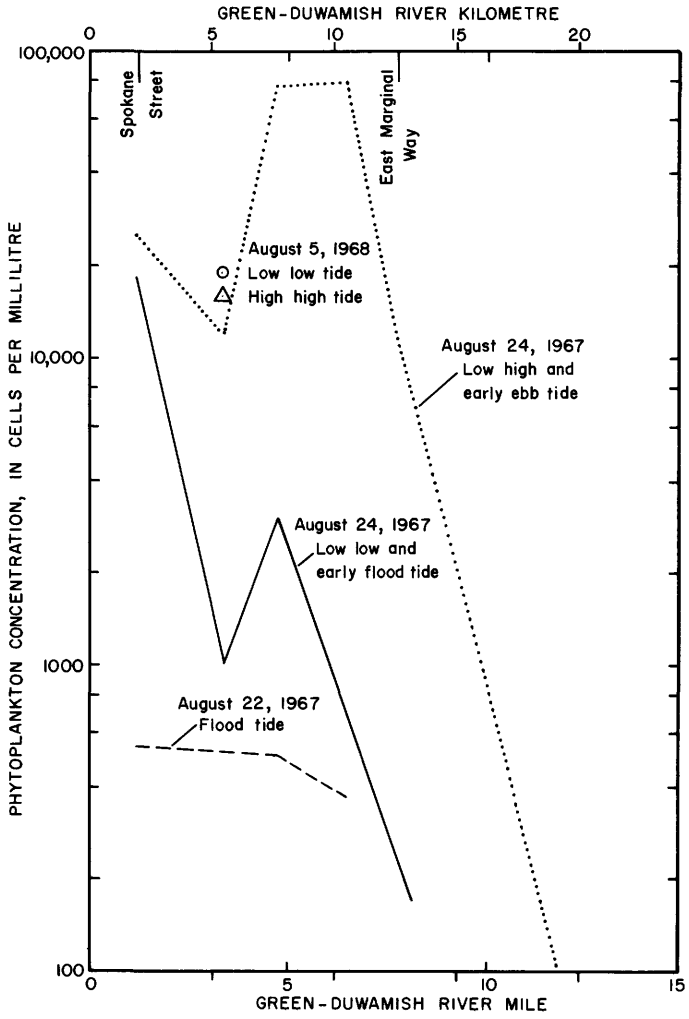

FIGURE 26.—longitudinal distributions of oval flagellates during a bloom in 1967 and data at two points during a bloom in 1968.

Michaelis-Menton factor, F_N, for a particular nutrient is expressed in the form

$$F_N = \frac{C}{C+C_{½}}, \qquad (50)$$

where C is the concentration of the particular nutrient and $C_{½}$ is C when $F_N = ½$.

Existing literature does not provide values of $C_{½}$ for all phytoplankton taxa found in the Duwamish River estuary. However, likely ranges of $C_{½}$ for the types and sizes of phytoplankton in the estuary may be 0.01 to 0.1, 0.002 to 0.02, and 0.001 to 0.05 mg/l for nitrate nitrogen, ammonium nitrogen, and phosphate phosphorus, respectively. Especially helpful in providing these data were the reports by Eppley, Rogers, and McCarthy (1969), MacIsaac and Dugdale (1969), and the Lake Tahoe Area Council (1968–70). The midpoints of the likely ranges of $C_{½}$ for nitrate and ammonium are 0.055 and 0.011 mg/l, respectively; MacIssac and Dugdale (1969) reported respective values of 0.062 and 0.023 mg/l for natural marine communities growing in eutrophic conditions.

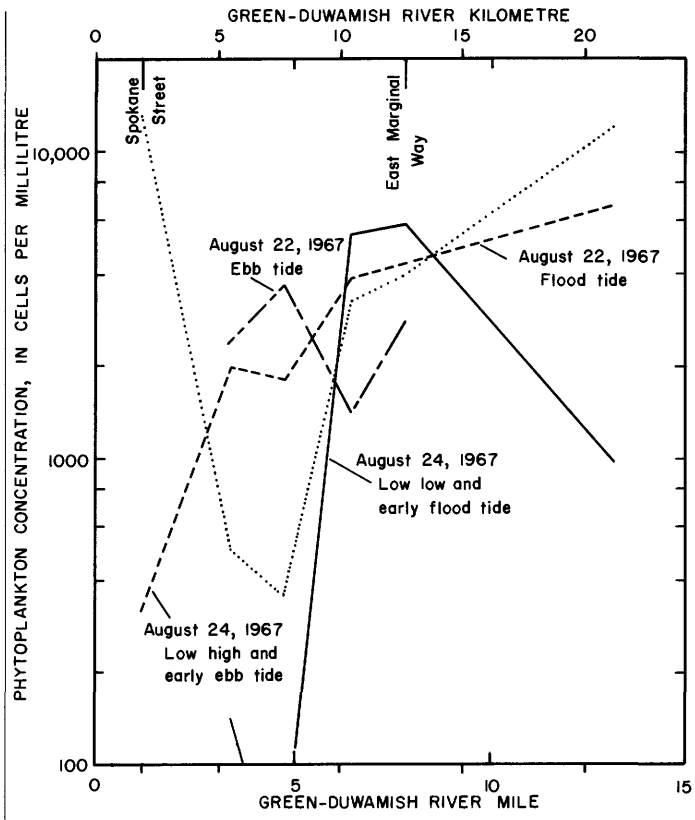

FIGURE 27.—Longitudinal distributions of "coccoids" plus "coccoid" clusters during a bloom in 1967.

Figure 29 shows the Michaelis-Menton factors for nitrate + nitrite and ammonium nitrogen and for phosphate phosphorus that were computed using equation 50 and midpoint values of the likely ranges of $C_{½}$. Nutrient-concentration data were available for 3-ft (1-m) depth samples collected semimonthly and monthly during most of the probable bloom periods, July-early September of 1967 and 1970–71 at East Marginal Way, 16th Avenue South, and Spokane Street Bridges. Analyses of these data indicate that (1) concentrations of ammonium nitrogen, NH_4-N; nitrate + nitrite nitrogen (NO_3+NO_2)-N; and total phosphate, PO_4-P, equaled or exceeded 0.25 mg/l in 79, 92, and 93 percent of the samples, respectively; and (2) variations in nutrient concentrations were unrelated to chlorophyll *a* concentrations. For a concentration of 0.2 mg/l, the curves in figure 29 give factors ranging from 0.79 to 0.95 times maximum growth. Two inferences important to the modeling and the management of the Duwamish River estuary may be implied from the foregoing analysis:

1. Given the present phytoplankton inflow to the Duwamish River estuary, present concentrations of nutrients in the estuary usually are sufficiently high to be considered nonlimiting to the growth of the phytoplankton;
2. Therefore, if the phytoplankton inflow to the estuary does not increase, future increases in nutrient concentrations in the estuary from additional RTP effluent or from other sources probably will not greatly increase the phytoplankton biomass in the estuary.

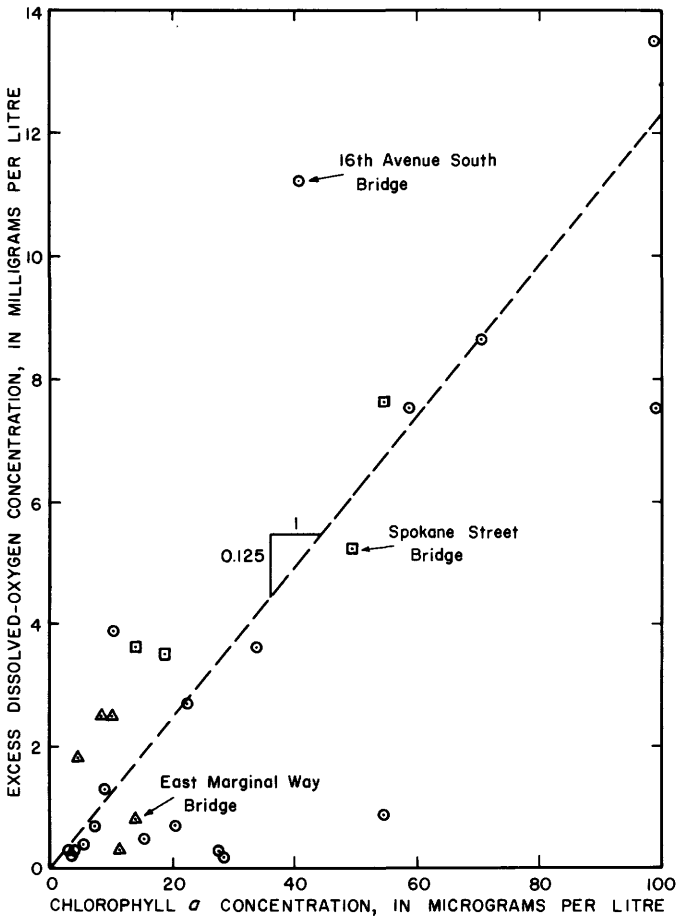

FIGURE 28.—Relation between concentrations of excess dissolved oxygen and chlorophyll *a* in some 3 ft (1-m) deep samples from three stations during 1967–68. Excess dissolved-oxygen concentration is the difference between sample concentration and a computed concentration for wedge and river water mixed in proportion to sample salinity.

The study of the effects of nutrients on phytoplankton growth rates in the Duwamish River estuary is continuing.

HERBIVORES

Herbivores are organisms that obtain their nourishment by consuming plants. Both freshwater and marine species were found in water samples taken from the Duwamish River estuary during periods of phytoplankton blooms in 1967 and 1968. Concentrations ranged from 0 to 110 herbivores/ml (table 13). These data suggest that concentration of herbivores and number of taxa tend to be higher in the water sampled from the two farthest downstream stations. Out of the seven freshwater taxa identified, rotifers, *Didinium nasutum, Vorticella* sp., and other ciliates were most often present in the samples. Twelve marine taxa were identified, of which holotrich spp., *Laboea conica,* and other heterotrich spp. occurred most often in the samples. The freshwater taxa were predominant in samples from the upstream stations, whereas marine taxa were predominant in samples from the downstream stations.

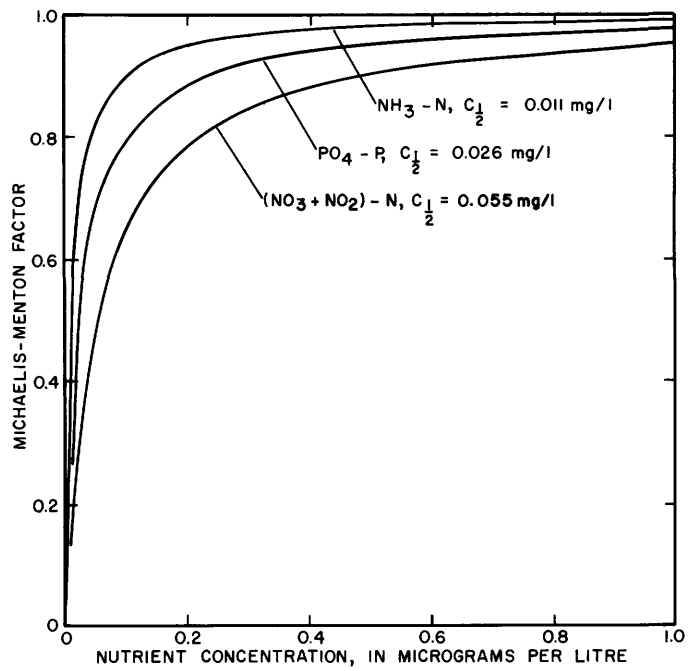

FIGURE 29.—Relations between Michaelis-Menton factors and concentrations of nutrients.

TABLE 13.—*Concentrations of herbivores in water samples from the Green-Duwamish River for 3 days during phytoplankton blooms in 1967 and 1968*

Date	Time (P.s.t.)	Sampling depth designation[1]	Taxa present[2]	Concentration (herbivores/ml)
Renton Junction Monitor				
1967				
Aug. 22	1530	Surface	F6, F7	1.1
24	1930	do	F6	.2
24	1540	do	F3, F6	6.8
East Marginal Way Bridge				
Aug. 22	0930	Surface	F4, F6	.4
22	1520	do	F6, F7	.1
24	0910	do	F4, F6, F7	.6
24	1525	do	F1, F4, F6, S12	.6
Boeing Bridge				
Aug. 22	0915	Surface	F1, S12	.4
22	1425	do	F4, F6	.3
24	0830	do	S4, S10, S11, S12	3.2
24	1440	do		0
16th Avenue South Bridge				
Aug. 22	0645	Surface	F2, S11, S12	2.8
22	1400	do	F1, F6, S12	.6
22	1405	Bottom	F1, F6, F7, S12	3.4
24	0805	Surface	S4, S12	1.8
24	0815	Bottom	F6, S8, S12	4.0
24	1415	Surface	F1, S12	.8
24	1425	Bottom	F5, S8, S12	7.3

TABLE 13.—*Concentrations of herbivores in water samples from the Green-Duwamish River for 3 days during phytoplankton blooms in 1967 and 1968*—Continued

Date	Time (P.s.t.)	Sampling depth designation[1]	Taxa present[2]	Concentration (herbivores/ml)
First Avenue South Bridge				
Aug. 22	0825	Surface	F1, S4, S11, S12	5.4
22	1340	------ do	F1, F4, S11, S12	2.8
22	1345	Bottom	S7, S12	1.7
24	0740	Surface	S4	13
24	0750	Bottom	S4, S8, S12	2.1
24	1345	Surface	F1, F6, S12	4.3
24	1355	Bottom	S11, S12	.7
Spokane Street Bridge				
Aug. 22	0735	Surface	F2, F7, S1, S6, S11, S12	3.6
22	0755	Bottom	F6, S5, S8, S12	16
22	1305	Surface	S3, S4, S12	8.0
22	1310	Bottom	F3, F6, S1, S5, S6	3.1
24	0645	Surface	S2, S4, S7, S12	110
24	0705	Bottom	F3, S2, S4, S7, S12	2.1
24	1310	Surface	F4, S12	12
24	1320	Bottom	S9	6.8
First Avenue South Bridge				
1968				
Aug. 5	0940	Surface	F7, S5, S12	8.9
5	1830	------ do	F4, F6, S5, S12	37

[1]Surface and bottom indicate samples from about 3 ft (1 m) below the water surface and about 3 ft (1 m) above the streambed, respectively.

[2]Herbivores counted and identified by W. A. Dawson are referred to by F (freshwater taxa) or S (saltwater taxa) and a number to indicate a specific taxa:F1-*Didinium nasutum*, F2-Nemata, F3-Rhizopoda and Actinopoda, F4-*Vorticella* sp., F5-Filamentous bacteria (decomposers), F6-Other ciliates, and F7-Rotifers; S1-Appendicularian ("Dikopleura"), S2-*Gyrodinium spirale*, S3-*Laboea strobila*, S4-*Laboea conica*, S5-*Laboea* sp., S6-Nauplius larvae, S7-*Noctiluca scintillans*, S8-*Parundella* sp., S9-*Strombidium* sp., S10-Copepodid larvae, S11-Holotrich spp., and S12-Other heterotrich spp.

☆ U.S. GOVERNMENT PRINTING OFFICE: 1976 - 690-036/94